THE UNIVERSITY OF ALBERTA

RESONANCE FLUORESCENCE STUDIES IN Cu^{63} AND Cu^{65}

by

DAVID CECIL SHERIFF WHITE

A THESIS

SUBMITTED TO THE FACULTY OF GRADUATE STUDIES

IN PARTIAL FULFILLMENT OF THE REQUIREMENTS FOR THE DEGREE

OF MASTER OF SCIENCE

DEPARTMENT OF PHYSICS

EDMONTON, ALBERTA

FALL 1971

ABSTRACT

A method of measuring lifetimes of excited nuclear levels has been developed using the resonance fluorescence technique. The method, using a continuous energy source of Compton scattered gamma rays, was applied to the measurement of the excited levels of Cu^{63} and Cu^{65} and lifetimes of several levels were calculated when and where statistical errors were small enough to give reliable results.

A complete review of the theory of the nuclear resonance fluorescence technique and the related experimental methods involved in the measurement of nuclear lifetimes are also included.

Acknowledgements

I would like to take this opportunity to thank several people whose help was essential in the completion of this thesis.

I am very grateful to Dr. D. M. Sheppard, my supervisor, for his help in the initial stages of the project, his final reading of the thesis and his encouraging remarks in my preparation for the oral exam.

I am especially thankful to Dr. B. Robertson for his encouragement and insistence throughout the project that the method should and would work even though at times I was very doubtful. I am indebted for the experience I have gained from him especially in the field of error calculations and the consideration of many aspects of the project which seemed almost trivial at first.

I also appreciate the help from Dr. S. Varma who assisted me at times when the derivation of formulae became difficult.

Thanks are also due to Con Green and his assistant Henry Nielsen for the many hours they spent in making the experimental apparatus.

To those members of the academic and technical staff who have made my stay at the Nuclear Research Centre very pleasant indeed, I also thank.

I wish to convey my special appreciation to an Edmonton firm, Electrical Industries, for their generous donation of 100lbs. of electrolytic copper without which this thesis would have been impossible.

I would like to thank my loving wife, Anna, for her consideration, support and her patience while I spent many late nights typing out this thesis with two fingers.

Finally, I wish to acknowledge the financial support provided by the University of Alberta throughout the course of this work.

TABLE OF CONTENTS

Page

INTRODUCTION 1

SECTION 1: THEORY OF RESONANCE FLUORESCENCE 3

DOPPLER EFFECT 4

SCATTERING EXPERIMENT 11

SELF ABSORPTION EXPERIMENT 18

TRANSMISSION EXPERIMENT 25

RESONANCE FLUORESCENCE TECHNIQUES 33

THERMAL METHOD 33

RADIOACTIVE SOURCES 39

CENTRIFUGE METHOD 42

NUCLEAR REACTIONS 45

BREMSSTRAHLUNG AND COMPTON SOURCES 49

SECTION 2: EXPERIMENTAL DETAILS AND RESULTS 54

EXPERIMENTAL ARRANGEMENT 54

EXPERIMENTAL PROCEDURE 60

EXPERIMENTAL RESULTS 70

DISCUSSION 74

REFERENCES 80

LIST OF FIGURES

Figure Page

1 $\psi(x,t)$ as a function of x for several values of t. 7

2 Effective temperature correction factor. 9

3 Experimental arrangement used for resonant scattering experiments. 11

4 Attenuation of the resonance scattering by Arsenic absorbers. 23

5 Resonance scattering from Li^7. 24

6 Schemmatic diagram of the apparatus used in the transmission experiment. 26

7 A plot of the function $F(n\sigma_{max})$. 29

8 A plot of $F(n\sigma_{max})$ for the lower range of $n\sigma_{max}$. 29

9 Effect of Doppler broadening upon the area above the transmission dip. 31

10 Effect of Doppler broadening upon the area above the transmission dip. 32

11 Doppler form of the emission and absorption lines. 34

12 Dependence of $\bar{\sigma}_{th}$ on the source temperature for different gamma ray energies. 37

13 Experimental arrangement for resonance scattering experiments using a heated radioactive source. 38

14 Temperature dependence of the resonance fluorescence effect from a source of As^{74}. 40

15 Influence of collisions in a As_4 source on the resonance effect. 41

16 Experimental arrangement for the scattering experiment using the centrifuge method. 42

Figure | Page

17 Dependence of the resonance effect on the source velocity for the 411kev level in Hg^{198}. 43

18 Dependence of the resonance effect on the source velocity for two excited levels in Sb^{121}. 44

19 Resonance fluorescence from the 2.14Mev level of B^{11}. 47

20 Resonance absorption of the 7.9Mev gamma rays from P^{31} as a function of angle. 48

21 Resonance absorption of the 12.33Mev gamma ray from Al^{27}. 48

22 Energy variation of gamma radiation undergoing Compton scattering. 50

23 The energy spread per unit angle of the Compton scattered radiation from a Co^{60} source. 51

24 Apparatus used to obtain a variable energy source of Compton scattered gamma rays. 52

25 Resonance fluorescence of the 0.77Mev level of Cu^{65} and the 0.439Mev level of Na^{23}. 53

26 Gamma ray spectrum from the Pu-Be source. 55

27 Schemmatic diagram of the experimental apparatus. 57

28 Gamma ray spectrum as seen through the lead cone. 59

29 Cu_{Fe} experimental run. 63

30 Cu_{Cu} experimental run. 64

31 Fe_{Fe} experimental run. 65

32 Fe_{Cu} experimental run. 66

33 $Cu_{Fe} - Fe_{Fe}$ background subtraction. 67

34 $Cu_{Cu} - Fe_{Cu}$ background subtraction. 68

35 Energy level configurations of Cu^{63} and Cu^{65}. 69

Figure Page

36 Graph of $\frac{t^3}{e^t - 1}$ vs. t. 71

LIST OF TABLES

Table Page

1 Tabulation of the function F. 14

2 Values of the constants δ, α and β. 17

3 Results of the gamma ray attenuations obtained for the comparison scatterer iron compared to that of the resonant scatterer copper. 58

4 Experimental results. 73

INTRODUCTION

The study of nuclear resonance fluorescence provides one with very useful information concerning the transition probability of fast gamma ray transtions, whose lifetimes are beyond the range of the delayed coincidence methods, that is shorter than 10^{-10} to 10^{-11} secs. The sensitivity of the resonance fluorescence method increases with decreasing lifetime i.e. with increasing level width. Although only transitions leading to the ground states of stable nuclei can be studied, the knowledge of the branching between competing gamma ray transitions will allow one in some cases to draw conclusions concerning transitions between excited states.

In addition to the information concerning transition probabilities obtained from the magnitude of the resonance effect, the study of the angular distribution of the resonant radiation represents a direct way of determining spins of excited states, multipole orders of transitions, and mixing ratios in the case of mixed transitions.

The resonance fluorescence technique of measuring level widths was proposed long before experiments were done on the subject because recoil energy losses upon emission and absorption of radiation presented the main obstacle to using a given isotope as the source of exciting radiation and as the scattering material. It was not until the 1950's with the advent of ultra-centrifuges that the emission and absorption lines could be made to coincide by the Doppler shift of the emission line, and thus a measurable resonance fluorescence effect could be observed. Even today, the main drawback to the resonance fluorescence technique is obtaining a source of radiation which satisfies

the necessary conditions for fluorescence.

In this thesis, the development of a new technique to measure lifetimes by the resonance fluorescence technique is described. The motive for the development was to find a method of measuring lifetimes which would substantiate results obtained by the Doppler Shift Attenuation Method and at the same time be independent of the 6 Mv van de Graaff accelerator at the University of Alberta. This was important since lengthy running times were expected in order to get good statistics.

The method is new in that a continuous energy source of Compton scattered gamma rays, obtained without the use of an accelerator as is the case for bremsstrahlung production, is used as the source of resonant radiation. This continuous energy source overcomes the problem of energy losses upon emission and absorption of radiation which proved the main obstacle in previous work on the resonance fluorescence technique.

The thesis is divided into two main sections. Since the theory of resonance fluorescence is insufficiently described in all papers, a complete literature search is necessary in order to obtain all the information needed to understand the theory. Also the nomenclature used by various authors is different and thus it was felt that a total review of the theory using a consistent notation would be very useful. The first section gives a review of the theory of resonance fluorescence and the experimental techniques involved. The second section describes the experimental method developed, the experiments carried out and the calculated results.

SECTION 1

THEORY OF RESONANCE FLUORESCENCE

For a photon of energy E, the cross-section for resonance fluorescence where direct gamma transitions to the ground state is the only mode of de-excitation, is given by Bethe and Placzek (1) for an isolated level as

$$\sigma^{o}(E) = \frac{\pi ƛ^{2}(2J_1+1)}{2(2J_o+1)} \frac{\Gamma^{2}}{(E-E_r)^{2}+\frac{1}{4}\Gamma^{2}} \qquad 1$$

where J_1 and J_o are the total angular momentum of the excited state and ground state respectively. The factor of two in the denominator expresses the multiplicity caused by the two possible independent polarisations of the photons.

If other de-excitation processes are possible, the total width of the excited state can be written as the sum of the partial widths

$$\text{i.e.} \quad \Gamma = \sum_{\iota} \Gamma_{\iota}$$

The cross-section for photoexcitation followed by the i^{th} mode of de-excitation is then

$$\sigma^{o}_{\iota}(E) = \frac{\pi ƛ^{2}(2J_1+1)}{2(2J_o+1)} \frac{\Gamma_o\Gamma_\iota}{(E-E_r)^{2}+\frac{1}{4}\Gamma^{2}} \qquad 2$$

Γ_o is the partial width for direct gamma ray transition to the ground state. Summing over all possible modes of de-excitation, the cross-section for resonance absorption is

$$\sigma^{o}_{ab}(E) = \frac{\pi ƛ^{2}(2J_1+1)}{2(2J_o+1)} \frac{\Gamma_o\Gamma}{(E-E_r)^{2}+\frac{1}{4}\Gamma^{2}} \qquad 3$$

DOPPLER EFFECT

The actual absorption lines are much wider than indicated by eq.3 because of the Doppler effect. The effective energy E' for a gamma ray, the absorbing nucleus moving towards the source of radiation with velocity v, is given by

$$E' = E(1 + \frac{v}{c})\surd(1 - \frac{v^2}{c^2})$$

$$\approx E(1 + \frac{v}{c}) \qquad 4$$

If the velocities of the nuclei in the absorber are assumed to be distributed according to a Maxwellian distribution function, the probability of a velocity component v in the direction of the source is

$$w(v)dv = \surd(M/2\pi KT) \exp(-Mv^2/2KT)dv \qquad 5$$

where M is the mass of the nucleus, K is Boltzmanns constant and T is the absolute temperature of the absorber. Now

$$dE' = \frac{E}{c} dv$$

and therefore the distribution of the effective energies is

$$w(E')dE' = \frac{c}{E}\left[\frac{M}{2\pi KT}\right]^{\frac{1}{2}} \exp\left[-\frac{M}{2KT}\left[\frac{(E' - E)c}{E}\right]^2\right] dE'$$

$$= \frac{1}{\Delta\surd\pi} \exp\left[-\left[\frac{(E' - E)}{\Delta}\right]^2\right] dE' \qquad 6$$

where $$\Delta = \frac{E}{c}\surd(2KT/M) \qquad 7$$

is the Doppler width. Writing eqs.1, 2, and 3 as

$$\sigma^0(E) = \sigma^0_{max}/\left[\left[2(E - E_r)/\Gamma\right]^2 + 1\right] \qquad 8$$

where σ^0_{max} refers to the values of the pure dispersion-form cross-section for $E=E_r$ in eqs.1, 2, and 3. To obtain the effective cross-section for gamma rays of energy E the above expression has to be averaged over all possible values of E'. Thus one obtains

$$\sigma(E,t) = \int \sigma^0(E')w(E')dE' = \sigma^0_{max}\,\psi(x,t) \qquad 9$$

where $x = 2(E - E_r)/\Gamma$, $t = 2\Delta/\Gamma$ and

$$\psi(x,t) = \frac{1}{\sqrt{\pi}\,t}\int_{-\infty}^{\infty} \frac{1}{1+y^2}\exp\left[-\frac{(x-y)^2}{t^2}\right] dy \qquad 10$$

where $y = 2(E' - E_r)/\Gamma$

$\psi(x,t)$ is in general a complicated function of x. However, simple expressions can be obtained for certain cases as shown by Bethe (2):

a) for t very small (purely natural width $\Gamma \gg \Delta$)

$$\psi(x,t) = \frac{1}{(1+x^2)} \qquad 11$$

and hence eqs.9 and 10 reduce to eq.8.

b) for t very large (pure Doppler width $\Delta \gg \Gamma$) and $x \ll t^2$

$$\psi(x,t) = \frac{\sqrt{\pi}}{t}\exp\left[-\frac{x^2}{t^2}\right] \qquad 12$$

c) for $x \gg t^2$ and any t

$$\psi(x,t) = \frac{1}{(1+x^2)} \qquad 13$$

d) for x = 0 (exact resonance) and any t

$$\psi(0,t) = \frac{\sqrt{\pi}}{t}\exp(t^{-2})\left[1 - \Phi(\tfrac{1}{t})\right] \qquad 14$$

where Φ is the Gaussian error function

$$\Phi(\tfrac{1}{t}) = \frac{2}{\sqrt{\pi}}\int_{o}^{\frac{1}{t}} \exp(-s^2)\, ds$$

In the special case of small t (natural width), eq.14 reduces to unity, meaning that in this case the cross-section at exact resonance is equal to σ^{o}_{max} . In the case of large t (Doppler width) one has

$$\psi(0,t) = \frac{\sqrt{\pi}}{t}$$

meaning that the cross-section at resonance is reduced to

$$\sigma_D(E_r) = \frac{\sqrt{\pi}}{2}\,\sigma^{o}_{max}\,\frac{\Gamma}{\Delta}$$

Since these integrations probably cannot be carried out analytically Melkonian *et. al.*(3) resorted to the use of series expansions and numerical methods. $\psi(x,t)$ may always be calculated from the convergent series

$$\psi(x,t) = \exp(-\frac{x^2}{t^2})\left[I_o + \frac{1}{2}(\frac{2x}{t^2})^2 I_1 + \frac{1}{4}(\frac{2x}{t^2})^4 I_2 + \ldots + \frac{1}{(2n)}(\frac{2x}{t^2})^{2n} I_n + \ldots\right]$$

where
$$I_o = \frac{\sqrt{\pi}}{t}\exp(t^{-2})\left[1 - \Phi(\tfrac{1}{t})\right]$$

$$I_1 = 1 - I_o$$

$$I_{n+1} = \frac{1.3.5\ldots(2n-1)t^{2n}}{2^n} - I_n \qquad \text{for } n>1$$

However, this series converges too slowly unless $\frac{2x}{t^2}$ is small. For large values of x and/or small values of t the semi-convergent series

$$\psi(x,t) = \frac{1}{1+x^2}\left[1 + \frac{t^2}{2}\,\frac{3x^2-1}{(1+x^2)^2} + \frac{3t^4}{4}\,\frac{5x^4-10x^2+1}{(1+x^2)^4} + \frac{15t^6}{8}\,\frac{7x^6-35x^4+21x^2-1}{(1+x^2)^6} + \frac{105t^8}{16}\,\frac{9x^8-84x^6+126x^4-36x^2+1}{(1+x^2)^8} + \ldots\right]$$

is convenient, but must be used with care. $\psi(x,t)$ for several values of t is shown in fig.1.

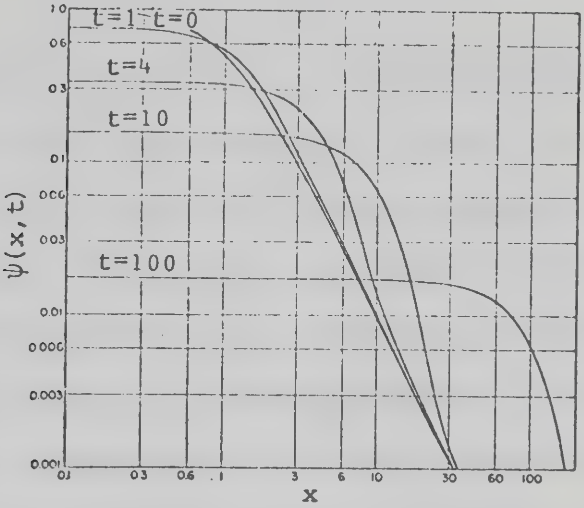

Fig.1. $\psi(x,t)$ as a function of x for several values of t. (Melkonian *et. al.* 1953.)

Since for the large majority of gamma ray transitions $\frac{\Delta}{\Gamma}>100$ one can use eq.12 and thus obtain for the cross-section

$$\sigma_D(E) = \sigma^0_{max}(\Gamma\sqrt{\pi}/2\Delta)\ \exp\left[-\left[\frac{(E - E_r)}{\Delta}\right]^2\right] \qquad 15$$

making eq.15 a very useful expression for the effective cross-section. Considering eq.9 and the fact that

$$\int_{-\infty}^{\infty} \psi(x,t)\ dx = \pi$$

it is clear that the integrated cross-section

$$\int \sigma(E,t)\ dE = \sigma^0_{max}\Gamma\pi/2 \qquad 16$$

does not depend on the relative size of the natural width and the

Doppler width. For the case of pure resonance fluorescence ($\Gamma_o = \Gamma$) it takes the form

$$\int \sigma(E,t)\, dE = \frac{2J_1 + 1}{2J_o + 1}\, \pi^2 \bar{\lambda}^2 \Gamma \qquad 17$$

In discussing the effect of the thermal motion of the absorbing nuclei the velocity distribution was assumed to be Maxwellian. This is a good assumption as long as gaseous materials are involved. However, in ordinary resonance experiments the absorbers are solids as well as the scatterers, and the question of the velocity distribution of the absorbing nuclei is more complicated. Lamb (4) has treated this problem in connection with neutron resonance experiments and his discussion also applies to the gamma ray problem. Provided that the crystal may be treated as a Debye continuum and that the lattice binding is weak

$$\text{i.e. } (\Delta + \Gamma) \gg 2K\Theta$$

where Θ is the Debye temperature, the absorption line was shown to have the same form as it would have in a gas at a temperature corresponding to the average energy per vibrational degree of freedom of the lattice. This means that in the expression eq.7 for the Doppler width one has to use an effective temperature T_{eff} which is some what higher than the actual temperature. The ratio of the effective temperature T_{eff} to the actual temperature T is, according to Lamb

$$\frac{T_{eff}}{T} = 3\left(\frac{T}{\Theta}\right)^3 \int_0^{\frac{\Theta}{T}} t^3 \left[\frac{1}{e^t - 1} + \frac{1}{2}\right] dt \qquad 18$$

Fig.2 shows the correction factor required in the expression for the Doppler width by taking into account the crystalline binding.

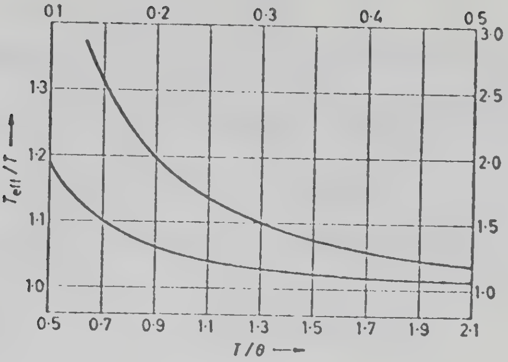

Fig.2. Correction factor taking into account the crystalline binding. The scales to the right and on top of the figure apply to the upper curve, those to the left and at the bottom apply to the lower curve. (Lamb 1939.)

The recoil energy losses upon emission and absorption of radiation present the main obstacle to using a given isotope as the source of the exciting radiation and as the scattering (absorbing) material. As long as the emitting and absorbing nuclei can be considered to be free the recoil energy loss in each process is

$$\Delta E = \frac{E_\gamma^2}{2Mc^2}$$

where M is the mass of the nucleus. Consequently, the line emitted from the same isotope is off resonance by an amount

$$\Delta E_r = \frac{E_\gamma^2}{Mc^2} \qquad 19$$

e.g. for a gamma ray of energy 500kev in a nucleus of atomic weight 100, $\Delta E_r = 2.68\text{ev}$
which is much larger than the expected natural width and also considerably larger than the Doppler width at room temperature.

$$\Delta = 0.37\text{ev}$$

Pollard and Alburger (5) derived the relation eq.19 in their first attempts at resonance fluorescence. Considering an energy level E and the emitted radiation of frequency ν_E from a nucleus of mass M, then by conservation of energy and momentum one obtains

$$Mv = \frac{h\nu_E}{c} \qquad \frac{Mv^2}{2} + h\nu_E = E \tag{20}$$

Substituting one into the other one then obtains

$$\frac{h^2\nu_E^2}{2Mc^2} + h\nu_E = E \tag{21}$$

and therefore the recoil energy is

$$E_r = \frac{h^2\nu_E^2}{2Mc^2}$$

$$= \frac{E_\gamma^2}{2Mc^2} \tag{22}$$

SCATTERING EXPERIMENT

The most common resonance fluorescence experiment with gamma rays is the scattering experiment. A typical experimental arrangement is shown in fig.3.

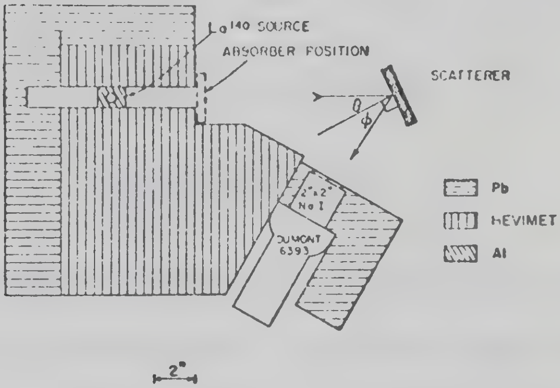

Fig.3. Experimental arrangement used for the resonant scattering experiments.

Unless the branching ratio to the ground state is small, this method affords the best discrimination against background radiation since the elastically scattered quanta rather than the inelastically scattered quanta is more easily detected.

The cross-section for elastic resonance is obtained from eq.2 by setting $\Gamma_1=\Gamma_o$. The thermal agitation is then taken into account using eq.9 and the effective cross-section becomes

$$\sigma_{sc}(E,t) = 2g\pi\lambdabar^2(\Gamma_o/\Gamma)^2\ \psi(x,t) \qquad 23$$

with
$$g = \frac{2J_1 + 1}{2J_o + 1}$$

For a thin scatterer, the number of scattered quanta is proportional to

$$S = \int N(E)\sigma_{sc}(E)\,dE \qquad 24$$

if N(E)dE is the number of gamma rays in the energy range dE present in the exciting beam. Provided N(E) is a slowly varying function of E as compared with the rapidly varying $\sigma_{sc}(E)$, eq.24 becomes

$$S = N(E_r)\int \sigma_{sc}(E)\,dE$$

$$= N(E_r)g\pi^2\lambda\!\!\!^{-2}(\Gamma_o^2/\Gamma) \qquad 25$$

which is independent of the Doppler width of the absorption line.

Because of the negligible variation of the electronic absorption cross-section σ_e over the range of interest in the integrations above, the 'shape' of the spectral distribution N(E) of the exciting radiation is not affected by the electronic attenuation in the scatterer and the scatterer may be treated as thin even if $n'D\sigma_e \gg 1$ as long as $nD\sigma_{ab}(E_r) \ll 1$ Here n'D is the total number of nuclei per sq.cm., and nD the number of resonant type nuclei per sq.cm. $\sigma_{ab}(E_r)$ is the effective peak resonance absorption cross-section.

If, on the other hand, $nD\sigma_{ab}(E_r)$ is not small compared with unity, the incident spectrum will be selectively depleted in the region of the absorption line as the beam penetrates into the scatterer and thus N(E) at a certain depth will be different in 'shape' from N(E) at the surface. The scatterer then has to be considered as thick and independent of the magnitude of the electronic attenuation.

If one assumes that $\Delta \gg \Gamma$ the effective cross-section has the Doppler form for pure resonance fluorescence i.e. $\Gamma = \Gamma_o$

$$\sigma_D(E) = \sigma^0_{max}\ (\Gamma\sqrt{\pi}/2\Delta)\ \exp\left[-((E - E_r)/\Delta)^2\right]$$

For a thick scatterer, the number of gamma rays scattered at a depth x out of an element dx by resonance fluorescence is

$$S(x)dx = ndx\int_0^\infty \sigma_D(E)N(E)\eta_e(E,x)\exp\left[-nx\sigma_D(E)\right]dE \qquad 26$$

where N(E)dE is the number of incident gamma rays at x=0 in the energy interval dE, n is the number of nuclei per cm^3 of the isotope under study and

$$\eta_e(E,x) = \exp(-\sum n_i\sigma_i x)$$

is the electronic attenuation. Expanding the exponential in eq.26 and making use of the slow variation with E of N(E) and $\eta_e(E,x)$ the integration over E can be carried out and one obtains

$$S(x)dx=ndx\sigma^0_{max}\ \frac{\sqrt{\pi}\Gamma}{2\Delta}\ N(E_r)\eta_e(E_r,x)\int_{-\infty}^{\infty}\exp\left[-\left[\frac{E - E_r}{\Delta}\right]^2\right]\sum\left[\frac{(-1)^m(nx\sigma_D(E))^m}{m!}\right]dE$$

$$=ndx\sigma^0_{max}\ \frac{\sqrt{\pi}\Gamma}{2\Delta}\ N(E_r)\eta_e(E_r,x)\int_{-\infty}^{\infty}\exp\left[-\left[\frac{E - E_r}{\Delta}\right]^2\right]\sum\left[\frac{(-kx)^m}{m!}\left[\exp\left[-\left[\frac{E-E_r}{\Delta}\right]^2\right]\right]^m\right]dE$$

where $$k = \frac{n\sigma^0_{max}\sqrt{\pi}\Gamma}{2\Delta} = \frac{ng\lambda^2\Gamma}{4\sqrt{\pi}\Delta}$$

substituting $(E - E_r)/\Delta = t$ and hence $dt = dE/\Delta$ one obtains

$$S(x)dx = ndx\sigma^0_{max}\ \frac{\sqrt{\pi}\Gamma\Delta}{2\Delta}\ N(E_r)\eta_e(E_r,x)\int_{-\infty}^{\infty}\exp(-t^2)\left[\sum\frac{(-kx)^m\exp(-mt^2)}{m!}\right]dt$$

$$= dx\ N(E_r)\eta_e(E_r,x)\ k\Delta\int_{-\infty}^{\infty}\sum\frac{(-kx)^m\exp\left[-(m + 1)t^2\right]}{m!}\ dt$$

$$= dx\ N(E_r)\eta_e(E_r,x)\ \sqrt{\pi}k\Delta\left[\sum\frac{(-kx)^m}{m!\sqrt{(m + 1)}}\right] \qquad 27$$

In the above formulae g is the ratio of the statistical weights of the excited and ground states respectively, λ is the wavelength of the gamma radiation, Γ is the natural width of the excited state and Δ is the thermal Doppler width of the absorption line at the temperature T.

In order to obtain the number of quanta scattered from an actual scatterer into a detector, a numerical integration over the scatterer has to be carried out taking into account the fact that the scattered radiation will undergo additional electronic absorption, but will not be resonance scattered again because it is now off resonance due to recoil momentum losses.

The integration can be performed numerically and Ofer and Schwarzschild (6) have evaluated the sum

$$\sum \frac{(-kx)^m}{m!\sqrt{(m+1)}} \equiv F$$

for the range $0<kx<6$ and the results are given in table 1.

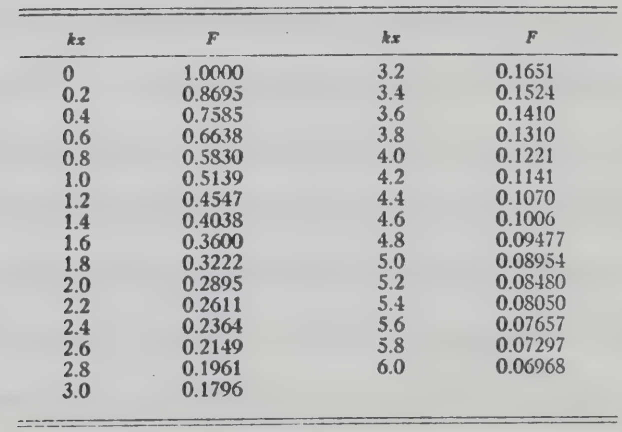

kx	*F*	*kx*	*F*
0	1.0000	3.2	0.1651
0.2	0.8695	3.4	0.1524
0.4	0.7585	3.6	0.1410
0.6	0.6638	3.8	0.1310
0.8	0.5830	4.0	0.1221
1.0	0.5139	4.2	0.1141
1.2	0.4547	4.4	0.1070
1.4	0.4038	4.6	0.1006
1.6	0.3600	4.8	0.09477
1.8	0.3222	5.0	0.08954
2.0	0.2895	5.2	0.08480
2.2	0.2611	5.4	0.08050
2.4	0.2364	5.6	0.07657
2.6	0.2149	5.8	0.07297
2.8	0.1961	6.0	0.06968
3.0	0.1796		

Table 1. Tabulation of the function F. (Ofer and Schwarzschild. 1959.)

An alternative to the numerical integration is to approximate the sum

by a function of kx which is easily integrated. An integrable approximation for the sum is given as follows;

$$\sum \frac{(-kx)^m}{m!\sqrt{(m+1)}} \approx \left[1 + \alpha kx + \beta(kx)^2\right] \exp(-\delta kx) \qquad 28$$

Thus one obtains for the yield of scattered quanta

$$S(b) = \int_0^b N(E_r)\eta_e(E_r,x)\sqrt{\pi}k\Delta \left[1 + \alpha kx + \beta(kx)^2\right] \exp(-\delta kx)\, dx$$

where b is the thickness of the scatterer. For the geometry shown in fig.3 and considering the distances travelled by the incident and scattered radiation in the scatterer

$$\eta_e(E_r,x) = \exp\left[-\left(\frac{n_1\sigma_1}{\cos\Theta} + \frac{n_1\sigma_2}{\cos\Phi}\right)x\right] \qquad 29$$

and kx is replaced by kx/cosΘ where n_1 is the total number of nuclei per cm^3 in the scatterer, σ_1 and σ_2 are the cross-sections for electronic absorption on incidence and exit respectively. σ_1 is a good geometry electronic cross-section for the incident beam because even small angle Compton scattering will change the energy of the radiation sufficiently to eliminate it from the resonance region if it is originally in this region. However, in some experiments where the energy distribution of the incident gamma rays extends to higher energies far beyond the region of the absorption line i.e. for instance bremsstrahlung, Compton scattering, might change a quantum of higher energy into one of just the right (resonant) energy. While this possibility should always be considered, Metzger (7) found that its effect on the scattering experiment is usually negligible. Also, with the use of a comparison scatterer matched to give the same electronic cross-section as the scatterer being studied, any quanta Compton scattered into the resonance

region will appear as a background subtraction.

σ_2 is the poor geometry electronic cross-section which is used for the outgoing radiation because of the possibility of scattering-in. Metzger (7) states that in his experience that a 20% reduction of the Compton cross-section for the outgoing beam represents a good correction for scattering-in effects.

Thus the total number of resonantly scattered quanta S(b) from a scatterer of thickness b is given by the equation

$$S(b) = \int_0^b N(E_r)\sqrt{\pi}k\Delta\left[1 + \frac{\alpha kx}{\cos\Theta} + \frac{\beta(kx)^2}{\cos^2\Theta}\right]\exp\left[-\left[\frac{\delta k}{\cos\Theta} + \frac{n_1\sigma_1}{\cos\Theta} + \frac{n_1\sigma_2}{\cos\Phi}\right]x\right]dx$$

with the substitution

$$a = \frac{\delta k}{\cos\Theta} + \frac{n_1\sigma_1}{\cos\Theta} + \frac{n_1\sigma_2}{\cos\Phi}$$

the first integration becomes;

$$\int_0^b \exp(-ax)dx = (1 - \exp(-ab))/a$$

the second becomes;

$$\frac{\alpha k}{\cos\Theta}\int_0^b x\exp(-ax)dx = \frac{\alpha k}{\cos\Theta}\left[- b\exp(-ab)/a + (1 - \exp(-ab))/a^2\right]$$

and finally the third becomes;

$$\frac{\beta k^2}{\cos^2\Theta}\int_0^b x^2\exp(-ax)dx = \frac{\beta k^2}{\cos^2\Theta}\left[-b^2\exp(-ab)/a - 2b\exp(-ab)/a^2 + 2(1-\exp(-ab))/a^3\right]$$

Thus the total resonant yield is;

$$S(b) = N(E_r)\sqrt{\pi}k\Delta\ \frac{1}{a}\left[1 + \frac{\alpha k}{a\cos\Theta} + \frac{2\beta k^2}{a^2\cos^2\Theta} - \exp(-ab)\left[1 + \frac{\alpha kb}{\cos\Theta} + \frac{\beta k^2b^2}{\cos^2\Theta}\right.\right.$$

$$+ \frac{\alpha k}{a\cos\Theta} + \frac{2\beta k^2 b}{a\cos^2\Theta} + \frac{2\beta k^2}{a^2\cos^2\Theta} \Bigg]\Bigg] \qquad 30$$

Table 2 gives sets of values of the constants δ, α and β for use in eq.30. If $(kx)_{max}$ lies within the range indicated in the table, then the yield as calculated with the approximation of Ofer and Schwarzschild will be correct to better than the maximum inequality as given in the table.

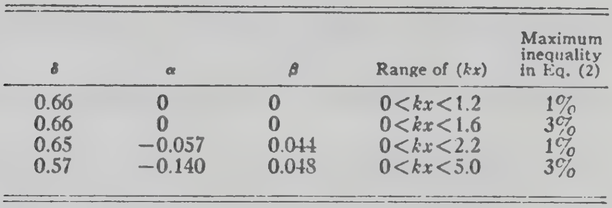

δ	α	β	Range of (kx)	Maximum inequality in Eq. (2)
0.66	0	0	$0<kx<1.2$	1%
0.66	0	0	$0<kx<1.6$	3%
0.65	−0.057	0.044	$0<kx<2.2$	1%
0.57	−0.140	0.048	$0<kx<5.0$	3%

Table 2. Values of the constants δ, α and β.(Ofer and Schwarzschild 1959.)

Since the conditions of many experiments lie within the range $0<(kx)_{max}<1.6$ then in these cases one can use the values $\alpha=0$, $\beta=0$ and $\delta=0.66$. Thus eq.30 reduces to the simple form

$$S(b) = N(E_r)\sqrt{\pi}k\Delta \, \frac{1}{a}\,(1 - \exp(-ab))$$

$$= \frac{N(E_r)\sqrt{\pi}k\Delta\left[1 - \exp\left[-\left[\frac{\delta k}{\cos\Theta} + \frac{n_1\sigma_1}{\cos\Theta} + \frac{n_1\sigma_2}{\cos\Phi}\right]b\right]\right]}{\frac{\delta k}{\cos\Theta} + \frac{n_1\sigma_1}{\cos\Theta} + \frac{n_1\sigma_2}{\cos\Phi}} \qquad 31$$

SELF ABSORPTION EXPERIMENT

The evaluation of the scattering experiment in terms of the level width is only possible if the shape of the incident gamma ray spectrum is known. Also a knowledge of the solid angle subtended by the scatterer at the detector and vice-versa plus the detector efficiency have to be known in order to calculate the number of resonance fluorescence gamma rays detected as a fraction of the total number of resonance gamma rays as given by eq.30.

When a nuclear reaction serves as the source of the exciting radiation $N(E_r)$ depends on the angular distributions and correlations of the reaction products, on the bombarding energy and thus on the target thickness and the excitation function. $N(E_r)$ is also affected by the slowing down and the scattering of the recoiling target nucleus prior to the emission of the gamma radiation. Thus the lack of knowledge of one or several of these factors affecting $N(E_r)$ becomes the source of considerable uncertainty in the determination of the width and hence the transition probability.

The dependence on $N(E_r)$ is avoided in a self absorption experiment first proposed by Metzger (7), in which one measures the fractional reduction

$$R = (N_{sc}(0) - N_{sc}(d))/N_{sc}(0) \qquad 32$$

of the resonance scattering effect brought about by the insertion of an absorber of thickness d into the incident beam, the absorber being of the same material as the resonant scatterer. However, the dependence on $N(E)$ is avoided only if $N(E)$ is a slowly varying function of E. Before R is calculated according to eq.32, the counting rate $N_{sc}(d)$,

observed with the scatterer and the absorber in place, has to be corrected for the non-resonant electronic attenuation. In actual practice the effect of the electronic attenuation is eliminated by measuring $N_{sc}(0)$ with an absorber made of a different element but giving rise to the same electronic attenuation.

Considering first the case of a thin scatterer and a thin absorber, with N(E) a slowly varying function of E, the self absorption is

$$R = \frac{\int N(E)\sigma_{sc}(E)dE - \int N(E)(1 - n_a\sigma_{ab}(E)d)\sigma_{sc}(E)dE}{\int N(E)\sigma_{sc}(E)dE} \qquad 33$$

$$= \frac{n_a d\int N(E)\sigma_{ab}(E)\sigma_{sc}(E)dE}{\int N(E)\sigma_{sc}(E)dE}$$

$$= \frac{n_a d\int \sigma_{ab}(E)\sigma_{sc}(E)dE}{\int \sigma_{sc}(E)dE}$$

$$= \frac{n_a d(\sigma^0_{ab})_{max}\int \psi(x,t_a)\psi(x,t_s)dx}{\int \psi(x,t_s)dx} \qquad 34$$

where d is the absorber thickness in cms., n_a is the number of resonant nuclei per cm^3 in the absorber and

$$\sigma(E) = \sigma^0_{max}\ \psi(x,t_i) \qquad i=s,\ a$$

where the subscript i has been introduced because the scatterer and the absorber may be at different temperatures and thus have different Doppler widths Δ_s and Δ_a respectively. If we assume that $\Delta_i \gg \Gamma$ then

$\psi(x,t_i)$ takes the form as given in eq.12.

$$\psi(x,t_i) = \frac{\sqrt{\pi}}{t_i} \exp\left[-\left(\frac{x}{t_i}\right)^2\right]$$

Substituting one obtains

$$\begin{aligned} R &= n_a d(\sigma^o_{ab})_{max} \frac{1}{t_a t_s} \int_{\infty}^{\infty} \exp\left[-\left(\frac{x}{t_a}\right)^2 - \left(\frac{x}{t_s}\right)^2\right] dx \\ &= n_a d(\sigma^o_{ab})_{max} \frac{\sqrt{\pi}}{\sqrt{(t_a^2+t_s^2)}} \\ &= \frac{n_a d\ g_1\ \lambda^2\ \Gamma_o}{4g_2 \sqrt{(\pi(\Delta_a^2+\Delta_s^2))}} \end{aligned} \qquad 35$$

where g_1 and g_2 are the statistical weights of the excited and ground states respectively. However, using the more general form of ψ as given in eq.10, the integral of the product of two Doppler integrals $\psi(x,t_i)$ was shown by Bethe and Placzek (1) to have the value

$$\frac{\pi}{2}\ \psi\left[0,(t_a+t_s)/4\right]$$

With this and putting $t_a = t_s = t$ eq.34 becomes

$$\begin{aligned} R &= n_a d(\sigma^o_{ab})_{max} \frac{1}{2}\ \psi(0,\tfrac{t}{2}) \\ &= \frac{n_a d\ g_1\ \lambda^2\ \Gamma_o\ \psi(0,\frac{t}{2})}{4g_2\ \pi\ \Gamma} \end{aligned} \qquad 36$$

However, this general form of the self absorption R is very rarely used because for a large majority of gamma ray transitions $\Delta/\Gamma > 100$ making eq.35 the more convenient expression.

For pure resonance fluorescence $\Gamma_o = \Gamma$ and thus it is seen from eq.35 that the main advantage of the self absorption experiment over the scattering experiment is its ability to yield the width in a

pure resonance fluorescence case with very little knowledge concerning the incident spectrum.

For thick scatterers and absorbers, R has to be calculated using the form given by eq.26 and the self absorption R is given by

$$R = \left[S(b) - S(b+d)\right]/S(b)$$

where b and d are the thicknesses of the scatterer and the absorber respectively. By analogy with eq.26

$$S(x+d)dx = ndx \int_0^\infty \sigma_D(E)N(E)\eta_e(E,x+d)\exp\left[-n\sigma_D(E)d\right]\exp\left[-nx\sigma_D(E)\right]dE \qquad 37$$

and following through the sets of eq.27 one obtains

$$S(x+d)dx = dx\ N(E_r)\eta_e(E_r,x+d)\sqrt{\pi}k\Delta\left[\sum \frac{(-1)^m\ k(x+d)^m}{m!\ \sqrt{(m+1)}}\right]$$

If one considers the same geometry as in fig.3

$$\eta_e(E_r,x+d) = \exp\left[-\left(\frac{n_1\sigma_1 x}{\cos\Theta}\right) - \left(\frac{n_1\sigma_2 x}{\cos\Phi}\right) - n_1\sigma_1 d\right]$$

and

$$S(b+d) = \int_0^b N(E_r)\sqrt{\pi}k\Delta\left[\sum\left[-k\left(\frac{x}{\cos\Theta}+d\right)\right]^m\Big/m!\sqrt{(m+1)}\right] \exp\left[-\left(\frac{n_1\sigma_1 x}{\cos\Theta}\right) - \left(\frac{n_1\sigma_2 x}{\cos\Phi}\right) - n_1\sigma_1 d\right]dx$$

Using the approximation of Ofer and Schwarzschild and since for the large majority of experiments $0<(kx)_{max}\leq 1.6$ then $\alpha=\beta=0$ one gets

$$S(b+d) = N(E_r)\sqrt{\pi}k\Delta\int_0^b \exp\left[-\left[\delta k\left(\frac{x}{\cos\Theta}+d\right)+\left(\frac{n_1\sigma_1 x}{\cos\Theta}\right)+\left(\frac{n_1\sigma_2 x}{\cos\Phi}\right)+n_1\sigma_1 d\right]\right]dx$$

$$= N(E_r)\sqrt{\pi}k\Delta\exp\left[-(\delta k+n_1\sigma_1)d\right]\int_0^b \exp\left[-\left(\frac{\delta k}{\cos\Theta}+\frac{n_1\sigma_1}{\cos\Theta}+\frac{n_1\sigma_2}{\cos\Phi}\right)x\right]dx$$

$$= \frac{N(E_r)\sqrt{\pi}\,k\Lambda\exp\left[-(\delta k+n_1\sigma_1)d\right]\left(1 - \exp\left[-\left(\frac{\delta k}{\cos\Theta} + \frac{n_1\sigma_1}{\cos\Theta} + \frac{n_1\sigma_2}{\cos\Phi}\right)b\right]\right)}{\frac{\delta k}{\cos\Theta} + \frac{n_1\sigma_1}{\cos\Theta} + \frac{n_1\sigma_2}{\cos\Phi}} \qquad 38$$

Comparing eq.31 and 38 it is seen that if a self absorption measurement is made, the yield is reduced by the factor

$$\exp\left[-(\delta k + n_1\sigma_1)d\right]$$

Thus the self absorption R is given by

$$R = 1 - \exp\left[-(\delta k + n_1\sigma_1)d\right]$$

The term $\exp(-n_1\sigma_1 d)$ gives the attenuation of the gamma rays in the absorber. However, when comparison scatterers and absorbers are used this term is omitted to give the self absorption R as

$$R = 1 - \exp(-\delta kd) \qquad 39$$

In the above formulae n_1 is the total number of nuclei per cm^3 in the resonant absorber. The effect of the non-resonant (electronic) attenuation of the incident beam is eliminated by performing the measurement of S(b) with a non-resonant absorber, which is matched to give the same electronic attenuation as the resonant absorber, in place of the resonant absorber. The two absorbers can be matched with the most appropriate gamma rays from the radioactive sources Cs^{137}, Mn^{54}, Na^{22} and Co^{60} so as to give the same electronic attenuation of the radiation passing through it. Generally measurements in an experiment are done in the following order;

a) Resonant scatterer and a non-resonant absorber

b) Resonant scatterer and resonant absorber

c) Non-resonant scatterer and one of the absorbers.

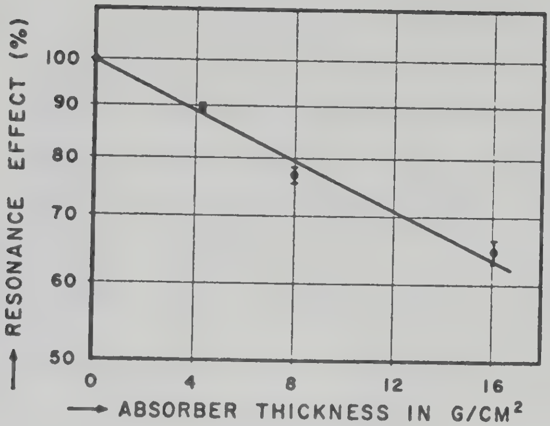

Fig.4. Attenuation of the resonance scattering from an arsenic scatterer by arsenic absorbers inserted between the source and scatterer. (Metzger 1957.)

Fig.4 shows the effect of placing resonant absorbers of different thicknesses between the source and the scatterer from the article by Metzger (Phys. Rev. 110.) Fig. 5 shows typical results of the self absorption experiment obtained by Rust *et. al.*(8) for resonance scattering from Li^7.

In a self absorption experiment the reduction of the resonance scattering by an absorber is studied. If this reduction, which usually amounts to only a small fraction of the scattering effect, is to be measured with meaningful accuracy, the initial resonance effect has to be large i.e. the lifetime of the transition has to be short. This means that the self absorption method is applicable to a more limited group of transitions than the scattering experiment. This is evident by the fact that the longest lifetime measured with the scattering method is $\sim 10^{-9}$secs, while the longest lifetime studied with the self absorption method is a few times 10^{-11}secs.

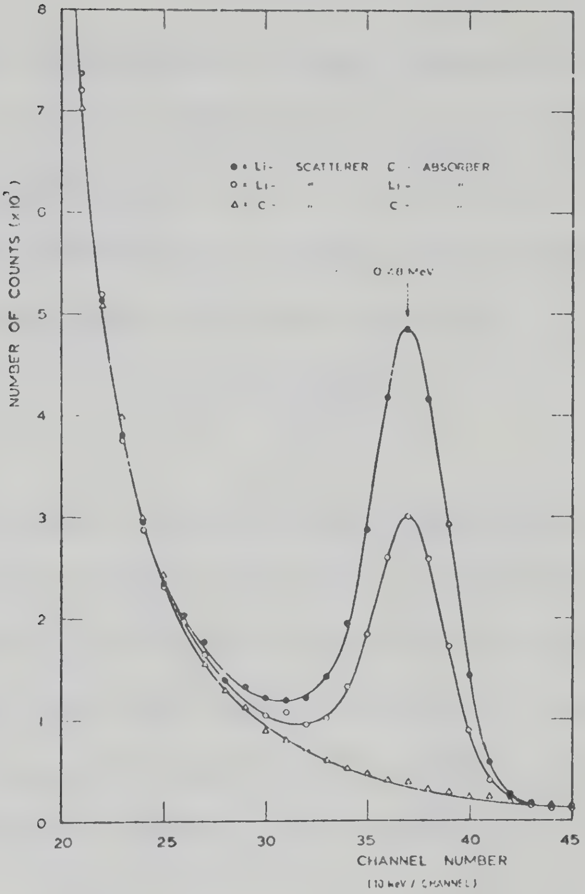

Fig.5. Resonance scattering from Li^7.(Rust *et.al.*1969.)

TRANSMISSION EXPERIMENT

In 1957 Smith and Endt (9) were successful in designing an experiment to measure lifetimes by using the transmission technique. Consider an excited nucleus in the target shortly after it has been formed by the absorption of a proton. It will be in motion in the direction of the proton beam with a velocity

$$v = \frac{\sqrt{(2E_p m_p)}}{M} \qquad 40$$

where M is the mass of the recoiling nucleus and m_p and E_p are the mass and kinetic energy of the proton, respectively. The high energy radiation emitted in the reaction studied is emitted long before any slowing down by collision can possibly occur. Upon emission at an angle α with respect to the direction of the nucleus, a gamma ray from a transition of energy E_o will receive an increment of energy

$$\Delta E_1 = (v/c)E_o\cos\alpha = E_o \frac{m_p}{M}\left[\frac{2E_p}{m_p c^2}\right]^{\frac{1}{2}} \cos\alpha \qquad 41$$

The energy which must be supplied externally in order that a photon may excite an identical nucleus to the same level as that from which it has been emitted is given by

$$\Delta E_2 = E_o^2/Mc^2 \qquad 42$$

This energy difference being the sum of the two equal parts, one representing the loss of energy to the recoil of the emitting nucleus and the other to the recoil of the absorbing nucleus. Resonance fluorescence will occur when $\Delta E_1 = \Delta E_2$

Thus equating eqs.41 and 42 one obtains for the resonant angle, α_r

$$\cos\alpha_r = E_o/\sqrt{(2E_p m_p c^2)} \qquad 43$$

The apparatus used to detect this absorption effect is shown schematically in fig.6.

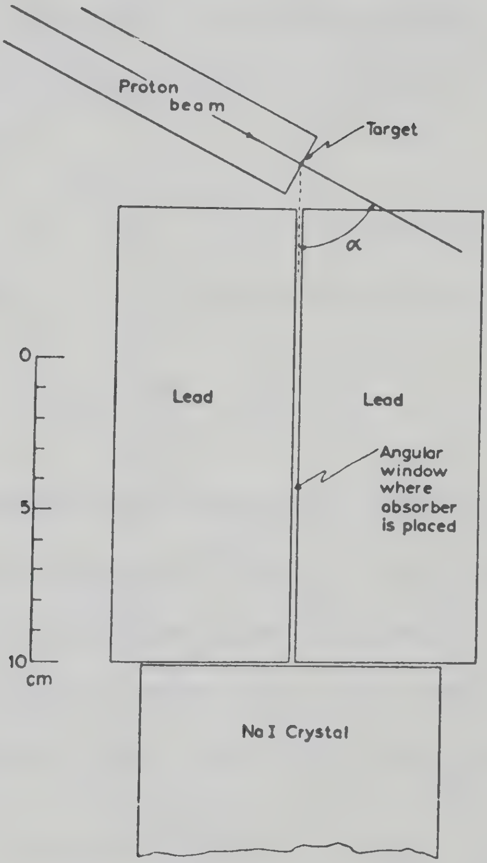

Fig.6. A schematic horizontal cross-section of the apparatus used to detect resonant absorption. (Smith and Endt 1958.)

The appropriate element is placed in the collimator opening and the intensity of the full-energy gamma rays is recorded as a function of angle. Defining the absorption integral

$$A_\alpha = \int_0^\pi A(\alpha)\, d\alpha = \int_0^\pi (1 - T(\alpha))\, d\alpha$$

where $A(\alpha)$ and $T(\alpha)$ are the absorption and the transmission, respectively at the angle α. The absorption $A(\alpha)$ can be written more explicitly as

$$A(\alpha) = \int_0^\infty (1 - \exp(-n\sigma_D(E)))\, f(E - E')\, dE \qquad 44$$

where E is the energy of a gamma quantum incident on the collimator slit, and n is the number of absorber nuclei per unit area. The average energy of gamma quanta incident on the slits follows from eqs.41 and 42 as

$$E' = E_0 - E_0^2/2Mc^2 + (v/c)E_0\cos\alpha \qquad 45$$

The function $f(E - E')$ is normalised so that

$$\int_0^\infty f(E - E')\, dE = 1$$

and is the energy distribution of the gamma quanta which would be transmitted through the collimator in the absence of an absorber. The width of this function (the instrumental width) is determined by the width of the collimator slit and by the angular divergence of the protons incident on the target. The absorption cross-section is

$$\sigma(E) = \frac{(2J_1+1)\,\lambda^2}{2(2J_0+1)\,4\pi} \quad \frac{\Gamma_{\gamma o}\Gamma}{(E - E_0')^2 + \frac{1}{4}\Gamma^2} \qquad 46$$

Γ and $\Gamma_{\gamma o}$ represent the total width of the excited state and the width for the ground state transition. Γ is used since one is not interested in the process de-exciting the absorbing nucleus, but only in the cross-section for the removal of photons from the beam. E_0' is the resonant energy such that

$$E_0' = E_0 + E_0^2/2Mc^2$$

The absorption integral can now be evaluated using eqs.44 and 46

$$A_\alpha = \int_0^\pi A(\alpha)\, d\alpha = \int_0^\infty dE(1 - \exp(-n\sigma(E))) \int_0^\infty f(E - E')\frac{d\alpha}{dE'}\, dE'$$

The factor $\frac{d\alpha}{dE'}$ is obtained by differentiating eq.45. As the integrand of the second integral differs from zero over a very narrow energy range this factor may be considered constant and is replaced by $(\frac{d\alpha}{dE'})_r$ at resonance, yielding

$$A_\alpha = (\frac{d\alpha}{dE'})_r \int_0^\infty (1 - \exp(-n\sigma(E)))\, dE \qquad 47$$

By substituting $x = 2(E - E_0')/\Gamma$

and

$$\sigma_{max} = \frac{(2J_1+1)\ \lambda^2\ \Gamma_{\gamma o}}{(2J_0+1)\ 2\pi\ \Gamma}$$

one obtains

$$A_\alpha = (\frac{d\alpha}{dE'})\ \frac{\Gamma}{2} \int_0^\infty (1 - \exp\left[-\frac{n\sigma_{max}}{1 + x^2}\right])dx \qquad 48$$

This integral appears in the analysis of neutron absorption curves and has been shown by von Dardel and Persson (10) to be expressible in terms of Bessel functions of the first kind with pure imaginary arguments. It is customary to denote these functions by

$$I_\nu(z) = \exp(-\tfrac{1}{2}i\pi\nu)\ J_\nu(iz)$$

where $J_\nu(z)$ is the Bessel function of the first kind. Applying the results of von Dardel and Persson to eq.48 one obtains

$$A_\alpha = (\frac{d\alpha}{dE'})_r\ \frac{\Gamma}{2}\ \pi\ F(n\sigma_{max}) \qquad 49$$

where $F(n\sigma_{max})$ is given by the formula

$$F(n\sigma_{max}) = n\sigma_{max}\exp(-\frac{1}{2}\,n\sigma_{max})\left[I_o(\frac{1}{2}\,n\sigma_{max}) + I_1(\frac{1}{2}\,n\sigma_{max})\right]$$

The function $F(n\sigma_{max})$ is plotted in figs.7 and 8.

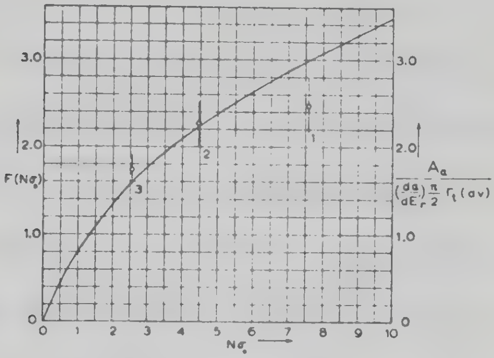

Fig.7. A plot of the function $F(n\sigma_{max})$.

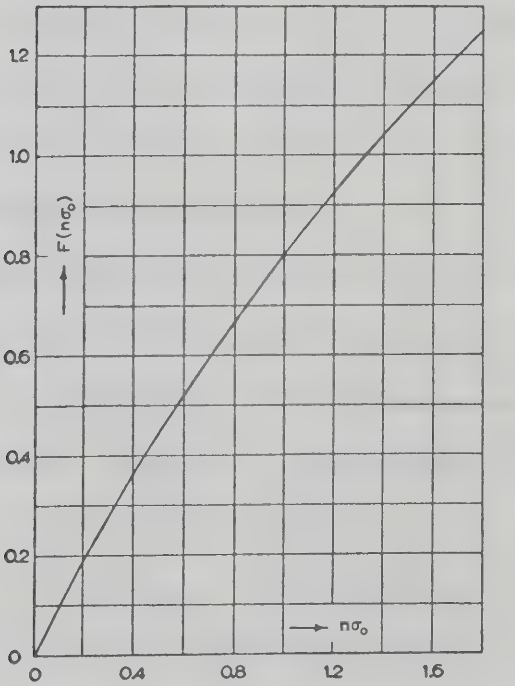

Fig.8. A plot of the function $F(n\sigma_{max})$ for the lower range of $n\sigma_{max}$.

If the ratio of the width $\Gamma_{\gamma o}/\Gamma$ is known then eq.49 can be used to find Γ and hence $\Gamma_{\gamma o}$. Also in principle it is possible to determine

Γ and $\Gamma_{\gamma o}$ from the variation of the absorption integral with absorber thickness since only one combination of Γ and $\Gamma_{\gamma o}$ can fit the curves above at two or more points.

In deriving eq.49 the thermal motion of the emitting and absorbing nuclei has not been taken into account. The thermal motion of the emitting nuclei merely contributes (negligible in this case) to the instrumental width. The thermal motion of the absorbing nuclei broadens the absorption line, however, and this reduces the peak cross-section. This has the effect of diminishing the self-absorption and thus of increasing the absorption integral. It is probably not possible to reduce the absorption integral to known functions when the correct Doppler broadened cross-section is substituted for that given in eq.46. However, Melkonian *et. al.*(3) have developed an approximation procedure for the analysis of neutron absorption integrals which can be adopted to find values of the level parameters in resonance absorption experiments.

In order to correct the values of the level parameters for the effect of thermal motion of the absorbing nuclei an approximate value of Γ is obtained by the method described above, on the assumption of no temperature motion. From this an approximate value of $t = \frac{2\Delta}{\Gamma}$ is calculated. From the curves of Melkonian *et. al.*, covering a large range of values of t and $n\sigma_{max}$, a correction is found which must be applied to the value of the absorption integral. A new value of Γ is then calculated and the procedure repeated until Γ reaches a stationary value.

In the curves of Melkonian *et. al.* the quantity D is defined by

$$D = ((A_\alpha)_D - A_\alpha)/A_\alpha$$

which gives the relative increase in area above the absorption curve arising from the Doppler effect.

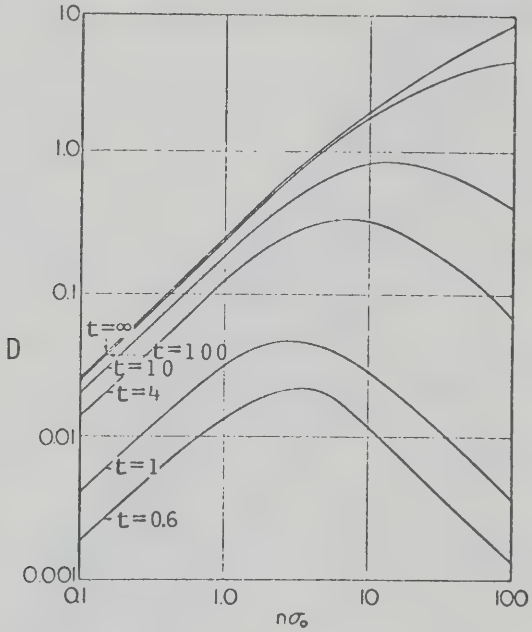

Fig.9. Effect of Doppler broadening upon the area above the transmission dip. (Melkonian *et. al.* 1953.)

From the above analysis it can be seen that no assumptions need be made about the resolution of the apparatus, or the angular distribution of the resonant scattering, in order to arrive at unique results for the level parameters. Thus the transmission experiment is a very useful one, however, since the source of exciting radiation is from (p,γ) reaction lifetimes of only high energy levels can be studied.

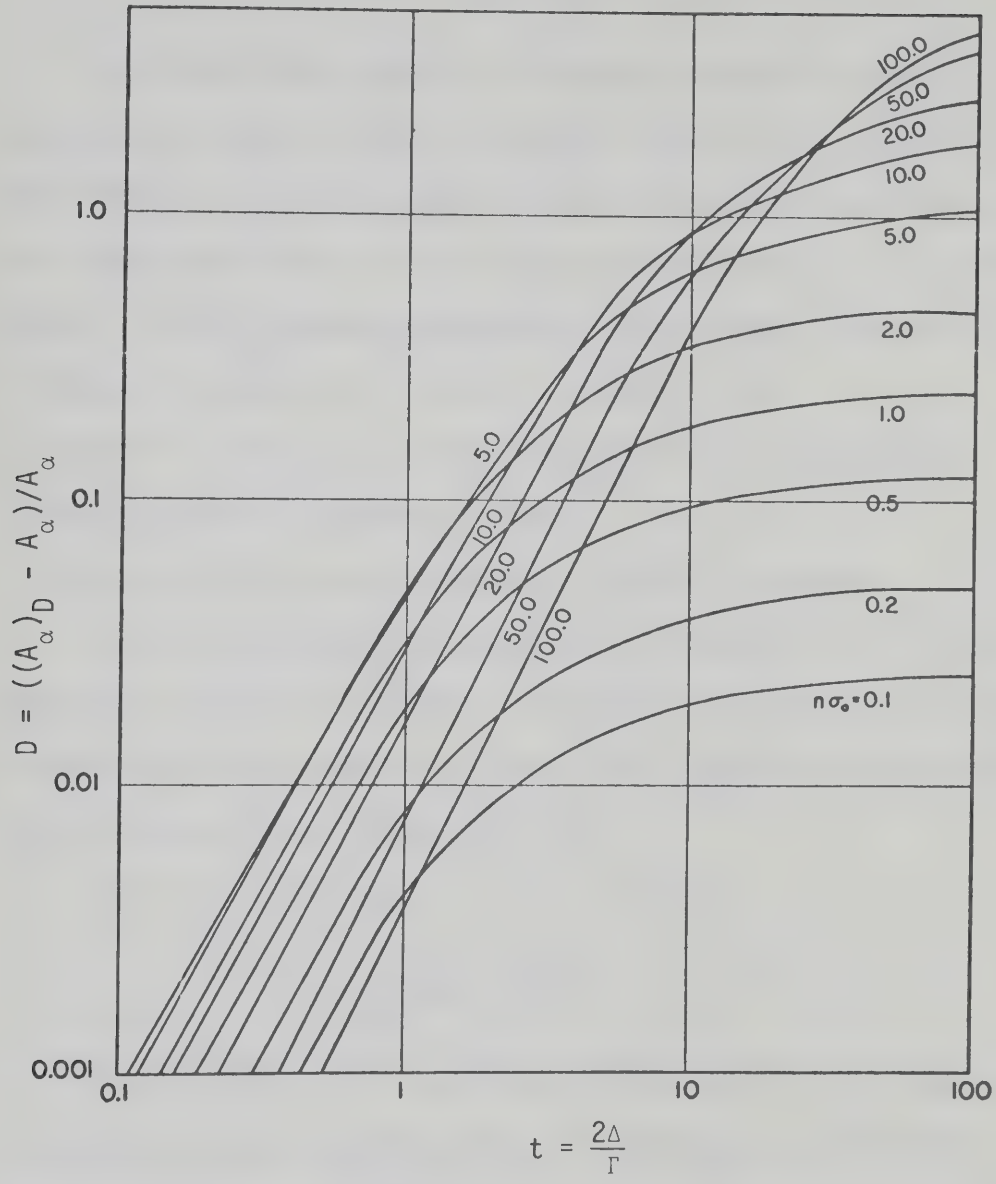

Fig.10. The effect of Doppler broadening upon the area above the transmission dip. D is plotted as a function of t for several values of $n\sigma_{max}$. (Melkonian *et. al.* 1953.)

RESONANCE FLUORESCENCE TECHNIQUES

The conditions under which nuclear resonance fluorescence can be observed are rather limited. In general terms, one may classify into four groups the various means by which the loss of energy upon emission and reabsorption due to recoil losses may be overcome to a sufficient degree to permit resonant absorption to take place. These are;

a) Doppler broadening by increase of temperature
b) Doppler broadening by previous emission and/or absorption
c) Doppler shift by mechanical motion
d) Doppler shift by previous emission and/or absorption.

In addition there is another class of experiment which uses a continuous source of radiation, bremsstrahlung emitted by a betatron. Classed within the same group is the use of Compton scattered radiation as the source of excitation radiation.

Each group will now be treated in turn.

THERMAL METHOD

This method, first introduced by Malmfors (11) in 1953, is based on the realisation that the overlap of emission and absorption line can be increased by increasing the Doppler width of either of these lines or both. For practical reasons the source is usually heated while the scatterer is kept at room temperature. The shape of the emission line and its position relative to the absorption line are depicted in fig.11 where E_e is the energy of the centre of the emission line and E_r the energy of the centre of the absorption line. If the source and the scatterer are at rest, $E_r-E_e= E_\gamma^2/Mc^2$, E_r being located

at $E_{level} + E_\gamma^2/2Mc^2$ and E_e at $E_{level} - E_\gamma^2/2Mc^2$. Clearly, the distribution of the exciting radiation is not wide compared with the absorption line, and for a thin target eq.24 has to be used. If Δ_e is the Doppler width of the emission line, the emission line has the pure Doppler form

$$N_D(E) = (N_o/\Delta_e\sqrt{\pi})\exp(-((E - E_e)/\Delta_e)^2) \qquad 50$$

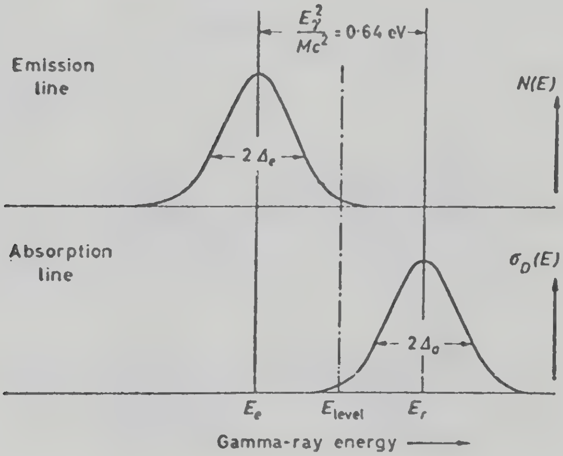

Fig.11. The Doppler form of the emission and absorption lines shows that the amount of overlap of the two lines is very small because of the recoil energy loss E_γ^2/Mc^2. (Metzger (7) 1959.)

Using eq.15 for the absorption line, the integration in eq.24 can be carried out.

$$S = \int N_D(E)\ \sigma_D(E)\ dE$$

$$= \frac{N_o\sigma^o_{max}\Gamma}{2\ \Delta_e\Delta_a} \int \exp(-((E - E_e)/\Delta_e)^2)\exp(-((E - E_r)/\Delta_a)^2)dE$$

$$= \frac{N_o\sigma^o_{max}\Gamma}{2\ \Delta_e\Delta_a} \exp\left(\frac{-E_e^2\Delta_a^2+E_r^2\Delta_e^2}{\Delta_a^2\ \Delta_e^2} \right) \int_{-\infty}^{\infty} \exp\left[-(\frac{E^2(\Delta_a^2+\Delta_e^2)-2E(E_e\Delta_a^2+E_r\Delta_e^2)}{\Delta_a^2\ \Delta_e^2} \right] dE$$

$$= \frac{N_o\sigma^0_{max}\Gamma}{2\,\Delta_e\Delta_a}\exp\left[-\frac{E_e^2\,\Delta_a^2+E_r^2\,\Delta_e^2}{\Delta_a^2\,\Delta_e^2}+\frac{(E_e\Delta_a^2+E_r\Delta_e^2)^2}{(\Delta_a^2+\Delta_e^2)\,\Delta_e^2\Delta_a^2}\right]\int_{-\infty}^{\infty}\exp\left[-\frac{E(\Delta_a^2+\Delta_e^2)-(E_e\Delta_a^2+E_r\Delta_e^2)}{\Delta_e\Delta_a\sqrt{(\Delta_a^2+\Delta_e^2)}}\right]^2 dE$$

substituting $E' = \dfrac{E\,(\Delta_a^2+\Delta_e^2) - (E_e\Delta_a^2 + E_r\Delta_e^2)}{\Delta_e\Delta_a\sqrt{(\Delta_a^2+\Delta_e^2)}}$

then $dE' = dE\,\dfrac{\sqrt{(\,\Delta_a^2+\Delta_e^2)}}{\Delta_e\Delta_a}$

and one obtains

$$S = \frac{N_o\sigma^0_{max}\Gamma}{2\sqrt{(\Delta_a^2+\Delta_e^2)}}\exp\left[-\frac{(E_e-E_r)^2}{\Delta_a^2+\Delta_e^2}\right]\int_{-\infty}^{\infty}\exp(-E'^2)\,dE'$$

$$S = \frac{N_o\sigma^0_{max}\Gamma\sqrt{\pi}}{2\sqrt{(\Delta_a^2+\Delta_e^2)}}\exp\left[-\frac{(E_e-E_r)^2}{\Delta_a^2+\Delta_e^2}\right] \qquad 51$$

Defining the average cross-section for the situation in fig.11 as

$$\bar{\sigma}(E_e) = \int N_D(E)\sigma_D(E)dE \Big/ \int N_D(E)dE \qquad 52$$

one obtains using eq.51

$$\bar{\sigma}(E_e) = \frac{\sigma^0_{max}\Gamma\sqrt{\pi}}{2\sqrt{(\Delta_a^2+\Delta_e^2)}}\exp\left[-\frac{(E_e-E_r)^2}{\Delta_a^2+\Delta_e^2}\right] \qquad 53$$

since the integration of $N_D(E)$ over E gives N_o. σ^0_{max} still refers to the peak value of the dispersive form cross-section in eqs.1, 2 and 3, and where Δ_a and Δ_e point out the possibility of having the scatterer and the source at different temperatures. It must be realised that the use of an average cross-section is only convenient for a thin scatterer for in thick scatterers $\bar{\sigma}$ would depend on the

thickness because of the change in N(E) through selective absorption. Comparing eqs.53 and 15 one notices that, for thin scatterers, the effect of the thermal agitation in the source may be taken into account by simply increasing the width of the absorption line to the value corresponding to the distribution of the thermal motion in the source and scatterer. In the general case represented in fig. 11, the exponential in eq.53 reduces $\bar{\sigma}$ to such a small value that the observation of resonance fluorescence is not possible in the presence of the usual background.

By setting $E_r - E_e = E_\gamma^2/Mc^2$ in eq.53 and by expressing the Doppler widths in terms of the corresponding temperatures, the average cross-section is brought into a convenient form for the thermal method;

$$\bar{\sigma}_{th} = \sigma^0_{max} \frac{\Gamma\sqrt{\pi}}{2E_\gamma} \left[\frac{Mc^2}{2k(T_a+T_e)}\right]^{\frac{1}{2}} \exp\left[-\frac{E_\gamma^2/Mc^2}{2k(T_a+T_e)}\right] \qquad 54$$

For a given transition $\bar{\sigma}_{th}$ reaches a maximum value if

$$k(T_a + T_e) = E_\gamma^2/Mc^2$$

i.e. if the Doppler width of the thermal motion equals the recoil energy loss

$$\Delta E_R = E_\gamma^2/Mc^2$$

The maximum value is then

$$(\bar{\sigma}_{th})_{max} = \sigma^0_{max}\, \Gamma\sqrt{\pi}\big/2\Delta E_R\sqrt{(2e)}$$

The ratio $\bar{\sigma}_{th}/(\bar{\sigma}_{th})_{max}$ is plotted in fig.12 versus the source temperature T_e, for different gamma ray energies, keeping T_a=300^{0}A and using an atomic weight of 200. From fig.12 one concludes that

the thermal method is most suitable for gamma ray energies between 150 and 450kev. For smaller energies the overlap of the emission and the absorption line is largest at room temperature and does not depend much on the source temperature. For energies above 450kev the overlap has not reached an appreciable value even at the highest temperatures conveniently reached with radioactive sources in the laboratory.

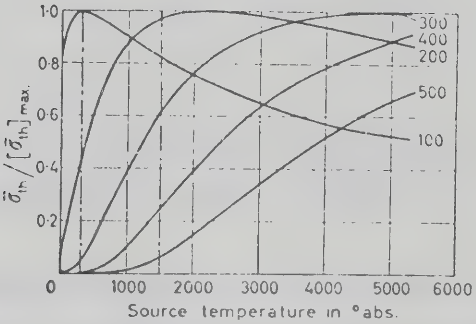

Fig.12. Dependence of $\overline{\sigma}_{th}$ on the source temperature for different gamma ray energies. The temperature of the scatterer is kept constant at 300^{0}A and the atomic weight of the element of interest is assumed to be 200. (Metzger (7) 1959.)

The typical experiment arrangement for the thermal method is shown in fig.13. Cylindrical ring scatterers are easy to build and afford rather uniform contributions of the different scatterer regions to the counting rate.

The resonance effects with the thermal method are rather small compared with the non-resonant background. The largest thermal effect observed so far amount to 15% of the background counting rate. Consequently, the matching of the comparison scatterers has to be done quite accurately. One should, for instance, attempt to choose

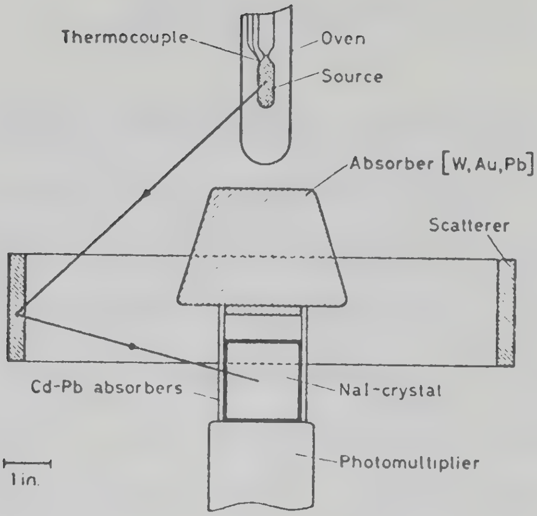

Fig.13. Experimental arrangement for resonance scattering experiment using a heated radioactive source. (Metzger (7) 1959.)

materials of comparable densities, otherwise the thickness of the matched scatterers is different and slight changes of the source position (thermal expansion, slight volatilisation and redeposition) will result in a mismatch which might be incorrectly attributed to resonance scattering.

RADIOACTIVE SOURCES

Several authors have suggested that the large velocities, imparted to the nucleus by the radiation preceding the gamma ray under study, could be utilised to restore the resonance conditions. However, initial experiments were unsuccessful, although the preceding beta decay had enough momentum to fully compensate for the recoil energy loss. The failure to observe resonance fluorescence was attributed to the slowing down of the recoiling nuclei by collisions suffered prior to the gamma ray emission. The collision times encountered lie between 10^{-13} and 10^{-15} seconds and thus the absence of a resonance effect establishes a lower limit of 10^{-12} to 10^{-13} seconds for the lifetimes of these gamma ray transitions.

The use of liquids and gaseous sources would increase the slowing down time and thus possibly be sufficient to observe resonance fluorescence. A typical experiment of this kind was performed by Metzger (12), who with gaseous sources of radioactive As^{72} and As^{74} utilised the beta decay to observe large nuclear resonance effects for the 835kev excited state of Ge^{72} and for the 596kev excited state of Ge^{74}.

For the scattering type of experiment the geometry similar to that used in the thermal method was employed. However, as long as one is restricted to temperatures below 1200^{0}C, only a few elements are sufficiently volatile for the present purpose. Thus one has to use compounds and among these hydrides are the best approximations to the free atoms, the mass of the hydrogen atoms being so small that the recoil velocities of the decaying nuclei are not much affected

by the presence or absence of the rest of the molecule. If hydrides are not suitable the halides are usually quite volatile.

Metzger, however, used a source of As_4 molecules. The gaseous form of the arsenic source was an essential condition for the observation of resonance fluorescence. This was demonstrated by the measurement of the temperature dependence of the resonance fluorescence effect. The results are shown in fig.14. Above $432^{0}C$, the temperature at which the arsenic was in the vapour phase, the effect is essentially constant. This fact is especially welcome for angular distribution experiments because it disposes of the necessity of rigid controls for the source temperature.

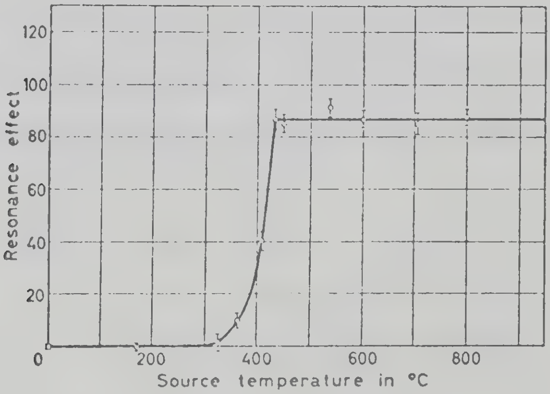

Fig.14. Temperature dependence of the resonance fluorescence effect from a source of As^{74}.The solid line represents the behaviour expected on the basis of vapour pressure data. (Metzger, 1956.)

Metzger also performed a series of experiments to show the influence of collisions in As_4 sources on the resonance effect. This was done by increasing the density of the As_4 vapour and the results are shown in fig.15.

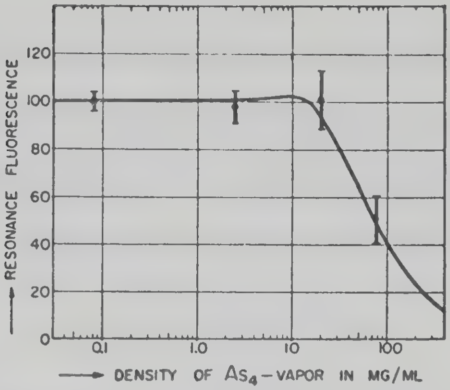

Fig.15. Influence of collisions in As_4 sources on the resonance effect from the 596kev level in Ge^{74}. The solid curve was calculated using a molecular diameter of 4.6×10^{-8}cm.

It is plainly seen that with the increase in density which thus leads to a decrease in the slowing down time of the recoiling nuclei there comes a point where the nuclei have slowed down so far that the gamma ray recoil energy losses cannot be compensated.

CENTRIFUGE METHOD

In this method one is dealing with radioactive nuclei which have loss all memory of the history leading to their formation i.e. they are in thermal equilibrium with the surroundings.

The recoil energy loss E_γ^2/Mc^2 corresponds to a Doppler velocity

$$v = (E_\gamma/Mc^2).c \tag{55}$$

For low energy gamma rays ($\leqslant$500kev) in heavy nuclei, this amounts to a few times 10^4cm/sec. Due to available materials it is seen from eq. 55 that the centrifuge method is restricted to low energy gamma rays ($\leqslant$500kev) and favour heavier nuclei.

Moon (13) in 1951 recognised the possibility of using an ultracentrifuge to realise the necessary mechanical velocities in a convenient way. The general experimental set-up is shown in fig.16 from the article of Metzger and Langhoff (14).

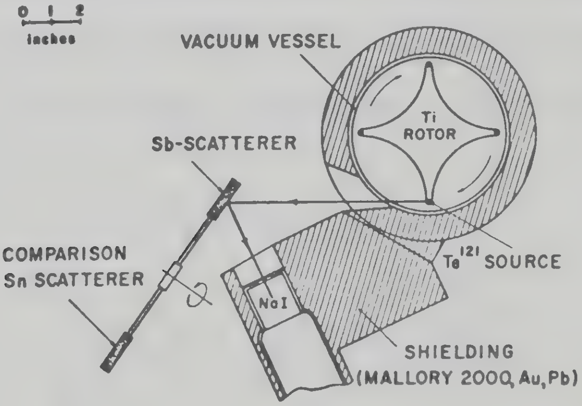

Fig.16. Experimental arrangement for the scattering experiments with the centrifuge method. (Metzger and Langhoff 1963.)

Provided that the tensile strength of the rotor material is sufficiently large, the emission and absorption lines can then be made to coincide,

giving rise to the largest possible resonance fluorescence effect. In practice, a finite cone of emission angles has to be accepted and the emission line is correspondingly broadened. As any deviation from the tangential direction results,in a lower velocity component, the average energy of the gamma rays hitting the scatterer will be somewhat reduced and thus a slightly higher peripheral speed will be necessary to achieve the best overlap.

The dependence of the average cross-section on the peripheral velocity v_p is obtained from eq.53 by inserting

$$E_e = E_r - E_\gamma^2/Mc^2 + (v_p/c)E_\gamma$$

A plot of the experimental counting rates versus rotor speed for the 411kev level in Hg^{198} taken from the work of Davey and Moon (15) is shown in fig.17. Fig.18 shows the same situation but for the 506kev and 576kev level in Sb^{121} from the work of Metzger and Langhoff (14). In both cases the curve drawn through the experimental points was calculated on the basis of free recoils and using Doppler widths corresponding to the actual temperatures of the source and scatterer.

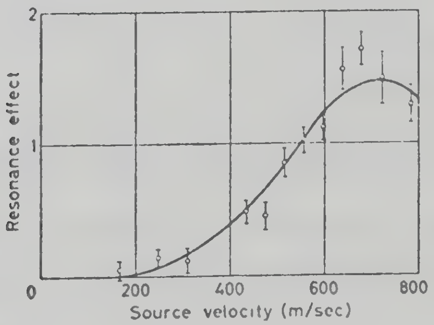

Fig.17. Dependence of the resonance fluorescence effect on the source velocity for the 411kev level in Hg^{198}.(Davey and Moon 1953.)

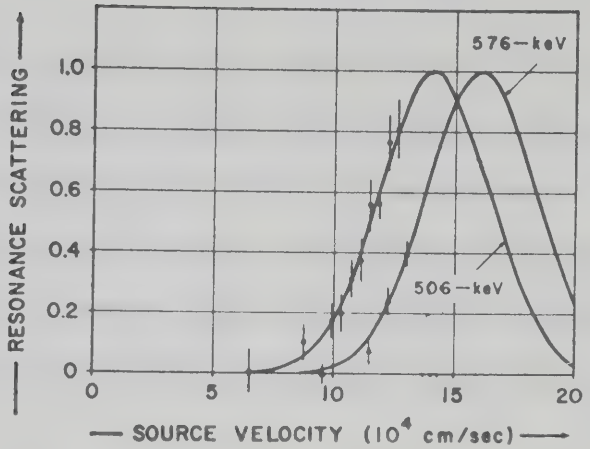

Fig.18. Dependence of the resonance scattering on the source velocity. Circles refer to the 506kev radiation, triangles to the 576kev radiation from excited levels in Sb^{121}.(Metzger and Langhoff 1963.)

The main problems of the centrifuge method involve the stability of the rotor motion, the tensile strength of the rotor and the high source strength necessitated by the small cyclic duty and the poor geometry. The main advantage of the centrifuge method is the high 'signal to noise' ratio that can be achieved. If the room background is considerable, the 'signal to noise' ratio can be improved if the detecting system is gated as in the article by Metzger and Langhoff. The gate was initiated by a light beam reflected into a photomultiplier tube by a mirror mounted on the drive shaft of the centrifuge. A properly placed second photomultiplier turned off the gate. In this way the analysers were gated everytime the source moved into the region where the direction of the emission of the gamma rays striking the scatterer subtended an angle of less than 30^0 with the tangent to the source path.

NUCLEAR REACTIONS

Nuclear reactions in light nuclei are convenient sources of gamma radiation for resonance fluorescence studies. Because of the higher excitation of the levels, a large fraction of the gamma ray transitions are sufficiently short lived to exhibit Doppler broadening even for solid targets since the recoiling nucleus will have not suffered collisions with the target material before emitting the gamma ray.

This Doppler broadening and shift of the emitted gamma rays is often orders of magnitude larger than would be needed for the compensation of the gamma recoil energy losses. This is a serious handicap as far as background is concerned, but it is, on the other hand, of considerable advantage because it allows the excitation of levels in other nuclei which fall into the energy region covered by the emitted spectrum.

If the lifetime of a level is such that some slowing down of the excited nuclei in the target material takes place before the emission of the gamma radiation, a self absorption experiment has to take the place of the scattering experiment because the exact shape of the energy distribution of the exciting radiation will be uncertain.

The excessive magnitude of the Doppler broadening in nuclear reactions results in a very low concentration of the resonant gamma rays and thus increases the importance of general and machine background.

However, a more important source of background are the neutrons created in the machine. These neutrons are captured by the materials surrounding the detector, giving rise to high energy capture radiation.

The reduction of the neutron background is one of the most important preliminary tasks before resonance fluorescence studies with nuclear reactions can be undertaken. Even for protons, which are the most favourable bombarding particles, the target materials have to be carefully selected, avoiding elements with low (p,n) thresholds.

The first resonance scattering experiments with a nuclear reaction as the source of the exciting radiation was carried out by Swann and Metzger (16) with the reaction $F^{19}(p,\alpha)O^{16}$. This reaction provided the source of two Doppler broadened lines of 6.91 and 7.12 Mev which were used to excite the corresponding states in O^{16}. In this case, since a considerable number of (p,α) reactions are exothermic and allow production of high energy gamma rays at moderate bombarding energies the neutron background is generally quite low.

Metzger, Swann and Rasmussen (17) used the inelastic scattering reaction $B^{11}(p,p')B^{*11}$ as the source of the Doppler broadened 2.14Mev gamma radiation to observe resonance fluorescence from the first excited state of B^{11}. The peculiarity of the (p,p') reaction is the possibility of self absorption in the target which was avoided with the (p,α) reactions where the target element differs from the element of the residual nuclei. For most nuclear resonance fluorescence experiments, the self absorption is rather small and the restrictions imposed on the source not severe.

Another problem of the (p,p') reaction is that the protons provide the major portion of the momentum and the excited nuclei are emitted in a forward cone. Since the gamma recoil energy losses are small compared to the momenta of the excited nuclei, the resonant

gamma rays for the element serving as the target material are emitted almost at 90^0 with respect to the direction of motion of the excited nuclei. Thus, there exists angular regions in which no resonant gamma rays are found and this severly restricts the choice of scatterer positions and renders angular distribution studies difficult. The situation is shown graphically in fig.19 from the article by Metzger, Swann and Rasmussen (17).

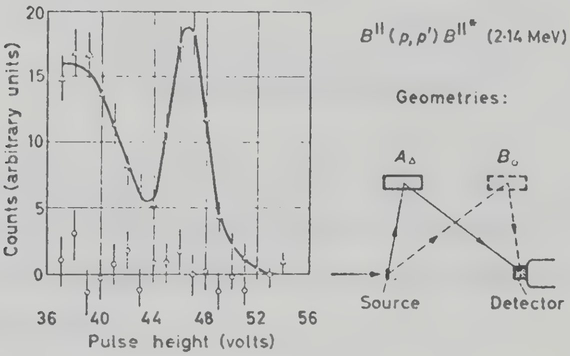

Fig.19. Resonance fluorescence from the 2.14Mev excited state of B^{11}. Triangles represent the pulse height distribution of the resonance radiation (position A). Circles were obtained with the scatterers placed in the non-resonant position B. (Metzger *et. al.* 1958.)

Smith and Endt (9) (18) have used gamma rays from proton capture for use in a resonance transmission experiment. The general theory of this method is given in the section on the transmission experiment. Figs.20 and 21 show typical transmission curves for resonance absorption using the experimental technique of Smith and Endt. In each case the absorption integral can be determined from these curves. The simplicity of the experimental arrangement and the modest bombarding energies make the proton capture process an attractive gamma ray source for resonance

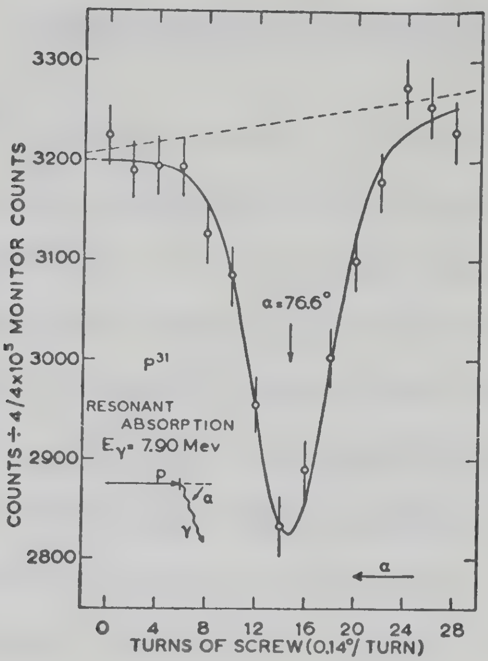

Fig.20. Resonant absorption of the 7.9Mev gamma rays from P^{31} as a function of angle. The arrow shows the centroid of the absorption peak, and the indicated angle is that calculated theoretically. (Smith and Endt 1958.)

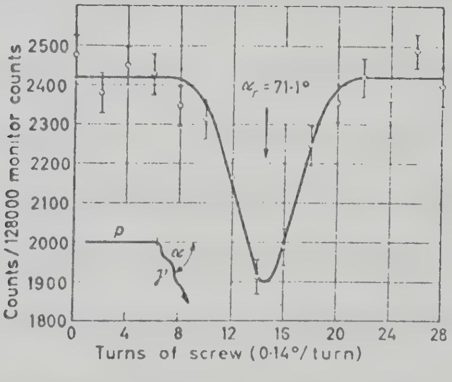

Fig. 21. Resonant absorption of the 12.33Mev gamma ray from Al^{27}. Si^{28} is the resonant material. (Smith and Endt 1958.)

transmission studies. Another advantage of this method is the freedom from assumptions regarding non-resonant scattering, and the spectral composition of the incident radiation which has permitted the attainment of low relative errors not easily obtained in other resonant experiments.

BREMSSTRAHLUNG AND COMPTON SOURCES

The first successful resonance fluorescence experiment using a continuous source of bremsstrahlung as the exciting radiation was performed by Hayward and Fuller (19). More recent work has been done by Beckman and Sandstrom (20) and Booth (21) (22).

The use of a continuous source of gamma rays introduces great difficulties due to background from competing scattering processes. However, among these inelastic Compton scattered radiation can be eliminated by choosing large scattering angles. Elastically scattered Rayleigh and Thompson radiations are not very intense with light nuclei since they are proportional to Z^3 and Z^4, respectively. For this reason all bremsstrahlung experiments have been performed with light nuclei such as C^{12} and Li^7.

Bremsstrahlung has advantages over gamma ray excitation, the main advantage being that no extra energy must be supplied to ensure resonance. The incident photon intensity varies slowly with energy and thus it is possible to calculate and measure it. The knowledge of N(E) was the main disadvantage of the scattering experiments and with bremsstrahlung this problem is overcome. A further advantage is that any level, including possible unknown levels, may be explored without the difficulty of finding gamma rays of sufficient relative intensity.

Cormack (23) suggested in 1954 that a gamma ray beam with an energy spread of a few kev and a mean energy which may be varied continuously could be obtained by the use of the Compton effect in a primary scatterer. Applying the laws of conservation of energy and momentum in the interaction of a gamma ray and a free electron,

the following expressions for the energy E of the Compton scattered radiation is obtained;

$$\frac{1}{E} = \frac{1}{E_0} + (1 - \cos\Theta)/m_0c^2 \qquad 56$$

where E_0 is the energy of the radiation incident on the scatterer, m_0 is the rest mass of the electron, and Θ is the angle in the laboratory space between the initial and final directions of the photon. Fig.22 illustrates the effect for the 1.33 and the 1.17Mev gamma rays from Co^{60}.

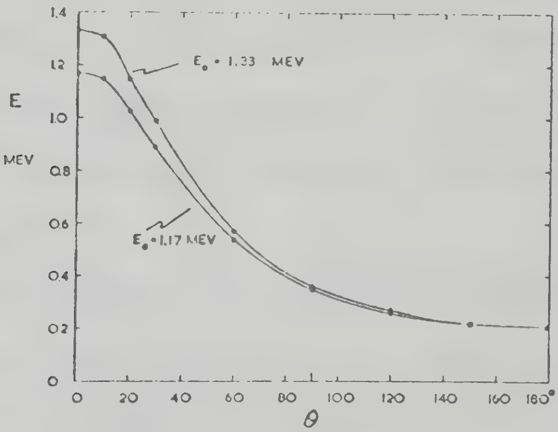

Fig.22. Energy variation of gamma radiation undergoing Compton scattering (Cormack 1954.)

The energy spread ΔE due to a spread in scattering angle $\Delta\Theta$ is given by the formula

$$\Delta E = \frac{(E_0^2/m_0c^2)\sin\Theta\,\Delta\Theta}{(1 + E_0(1-\cos\Theta)/m_0c^2)^2} \qquad 57$$

Fig.23 shows this energy variation per unit angle of Compton scattered radiation for the two gamma rays from Co^{60}.

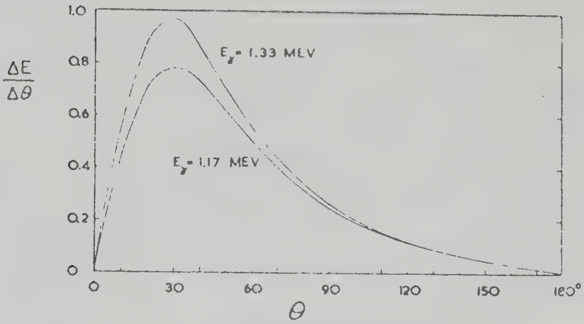

Fig.23. The energy spread per unit angle (Mev per radian) of the Compton scattered radiation as a function of the scattering angle for the gamma rays from a Co^{60} source. (Cormack 1954.)

Experiments using the Compton process, however, were not done until 1962 due to the non-availability of intense sources of gamma rays. The first was done by Mouton *et. al.*(24) followed in 1967 and 1968 by similar experiments performed by Tandon and McIntyre (25) and Rust *et. al.*(8)

Tandon and McIntyre (26) designed an apparatus to produce a variable energy gamma ray beam utilising gamma rays scattered by the Compton effect. The apparatus is shown in fig.24.

The Co^{60} source, the aluminium scatterer, and the target containing the nuclei to be studied are all placed on the circumference of a 2 metre radius circle. According to plane geometry all gamma rays leaving the Co^{60} source which scatter from the aluminium scatterer and strike the target will have scattered through the same scattering angle α. Thus all the gamma rays striking the target will have the same energy. This apparatus produced a gamma ray beam having an energy resolution of $\Delta E/E=2.5\%$ where ΔE is the full width at half maximum.

Using a similar form of apparatus but with a Co^{60} source of strength 4000 curies Rust *et.al.* obtained results shown in fig.5

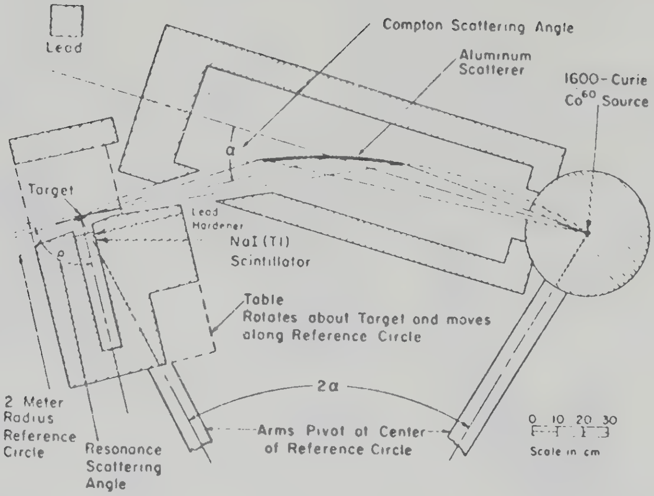

Fig.24. A scale drawing of the apparatus designed to obtain a variable energy source of Compton scattered gamma rays.(Tandon and McIntyre 1968)

and fig.25 for resonance absorption experiments on Li^7,Cu^{65} and Na^{23} respectively.

This method has advantages over the bremsstrahlung technique, for if the energy levels below the one of interest are excited by the more numerous low energy gamma rays of the bremsstrahlung further background will be introduced. Systematic errors in the lifetime measurements should, in principle, be smaller for the Compton scattering technique than for the bremsstrahlung technique. However, the energy range using the Compton method is limited and the bremsstrahlung technique is more versatile in this respect. Both techniques, however, suffer the problems of background from elastic Rayleigh and Thompson scattered gamma rays and thus they are restricted to studies in the low Z region.

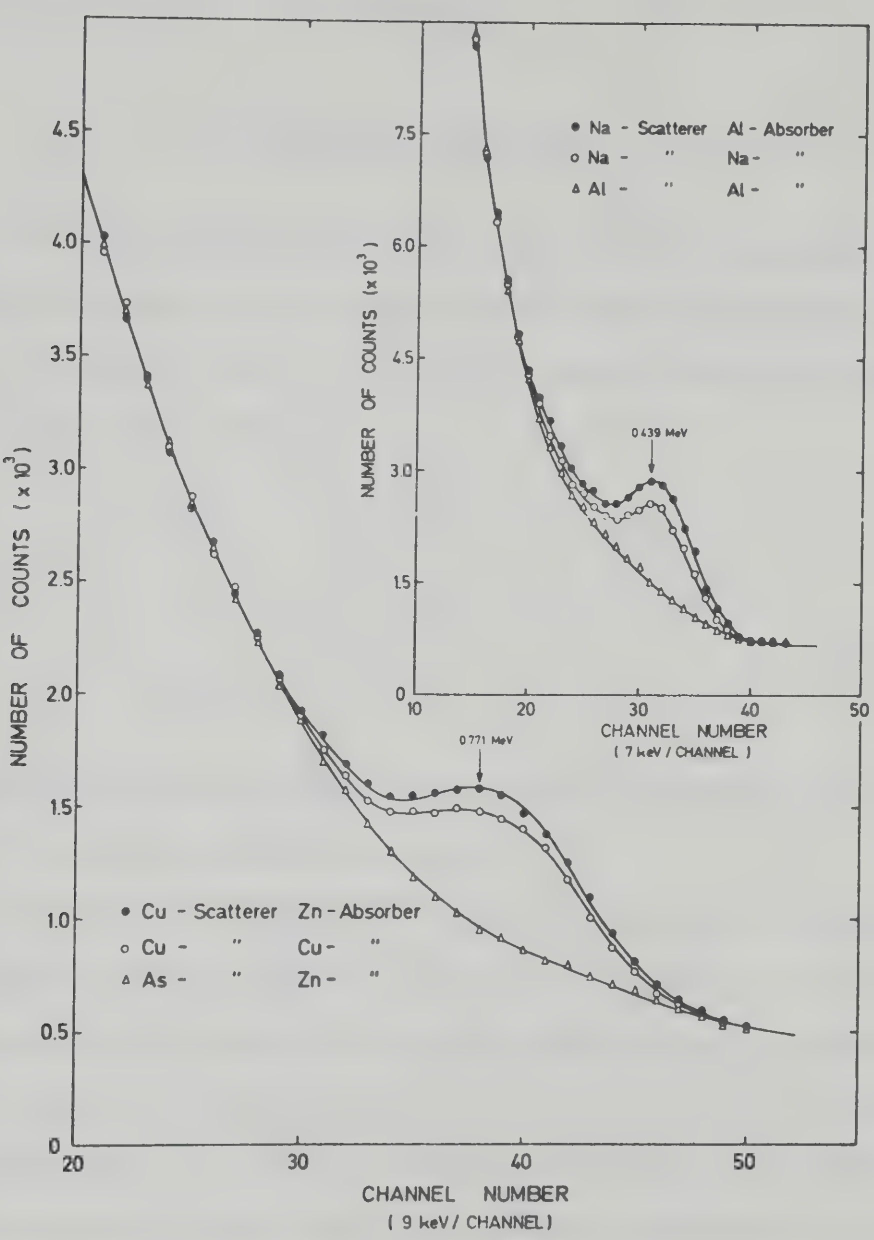

Fig.25. Results are shown for resonance fluorescence of the 0.771Mev level of Cu^{65} and the 0.439Mev level of Na^{23} using the Compton scattering technique. (Rust *et. al*.1969.)

SECTION 2

EXPERIMENTAL ARRANGEMENT

The experiment was performed using a plutonium-beryllium source placed in the centre of an aluminium drum, 20ins. in diameter, containing paraffin wax. The following reactions lead to the gamma ray spectrum seen in fig.26.

$$Pu^{232} \rightarrow \alpha + Th^{228} + \gamma$$

$$\alpha + Be^{9} \rightarrow C^{12} + n + \gamma$$

$$n + \underset{\text{paraffin}}{p} \rightarrow D^{2} + \gamma$$

Compton scattering of the gamma rays within the drum then leads to an effective continuous gamma ray source.

To estimate the Compton efficiency of the source the spectrum was compared with that of the $C^{12}(p,p')C^{*12}$ reaction carried out on the University of Alberta's 6 Mv van de Graaff at proton bombarding energy of 5Mev. Using the same Ge(Li) detector the peak to Compton of the 4.44Mev decay of C^{*12} was compared to that from the plutonium-beryllium source. It was found that the latter contained a sufficiently large increase in the Compton scattered gamma ray background to observe fluorescence.

In order to increase the Compton efficiency further experimental runs were done by placing nine different thicknesses of sheet aluminium (0.052ins. to 0.863ins.) between the source and the detector. However, it was found that the increase in the Compton efficiency was effectively nullified by the attenuation of the gamma rays by the

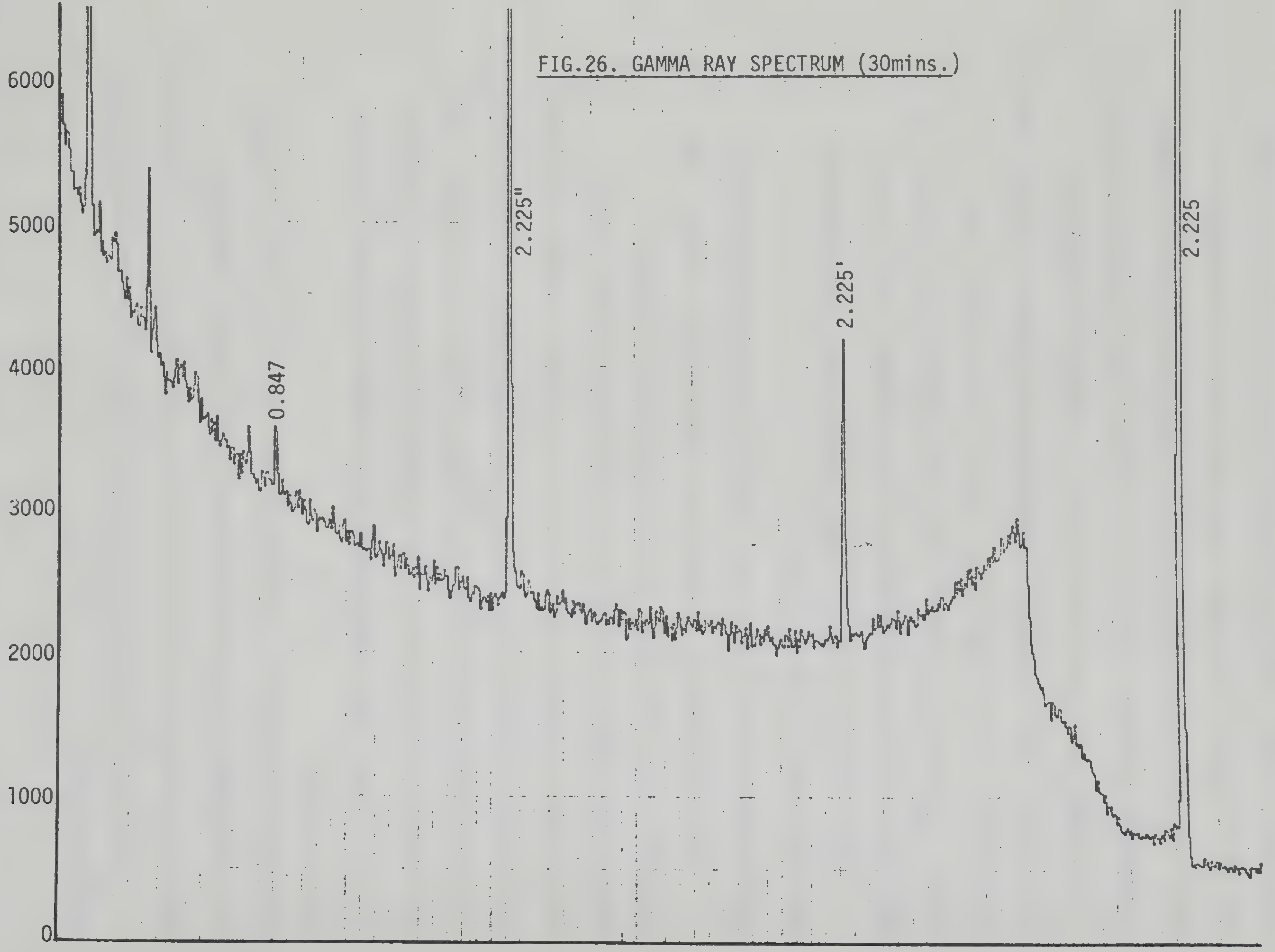

FIG.26. GAMMA RAY SPECTRUM (30mins.)

aluminium sheet.

The typical scattering experiment to observe resonance fluorescence would be impracticable in my case due to the effective size of the source i.e. the diameter of the aluminium drum. Thus the self absorption technique was adopted and the experimental apparatus is shown schemmatically in fig.27.

As can be seen a large absorber is necessary in order to shadow the scatterer from the source. This imposed a restriction on the type of resonant absorber and hence the resonant scatterer to be chosen. The two isotopes of copper, Cu^{63} and Cu^{65}, provide several excited nuclear levels whose lifetimes are known to be in the sub-picosecond region and hence in the range of application of the resonance fluorescence technique. Thus copper was chosen as the resonant scatterer.

Iron was chosen as the comparison scatterer and absorber since its electronic density and atomic Compton absorption cross-section is nearly the same as that of copper.

The thickness of the iron was so chosen that it had the same gamma ray electronic attenuation as that of copper. This was done using Co^{60} and Cs^{137} sources since their emitted gamma rays are off resonance for the excited levels of both copper and iron. Their energies also span the region of interest from 0.66Mev to 1.8Mev. Thus a good comparison could be obtained for the gamma ray electronic attenuation in copper and iron for the whole region of interest. Table 3 gives the results obtained for the best comparison between the copper and iron absorbers. The final column gives the ratio, expressed as a percentage, of $N_{Cu} - N_{Fe}$ to N_{Cu} where N_{Cu} and N_{Fe} are the total number of counts in the respective gamma ray peak of the source with the

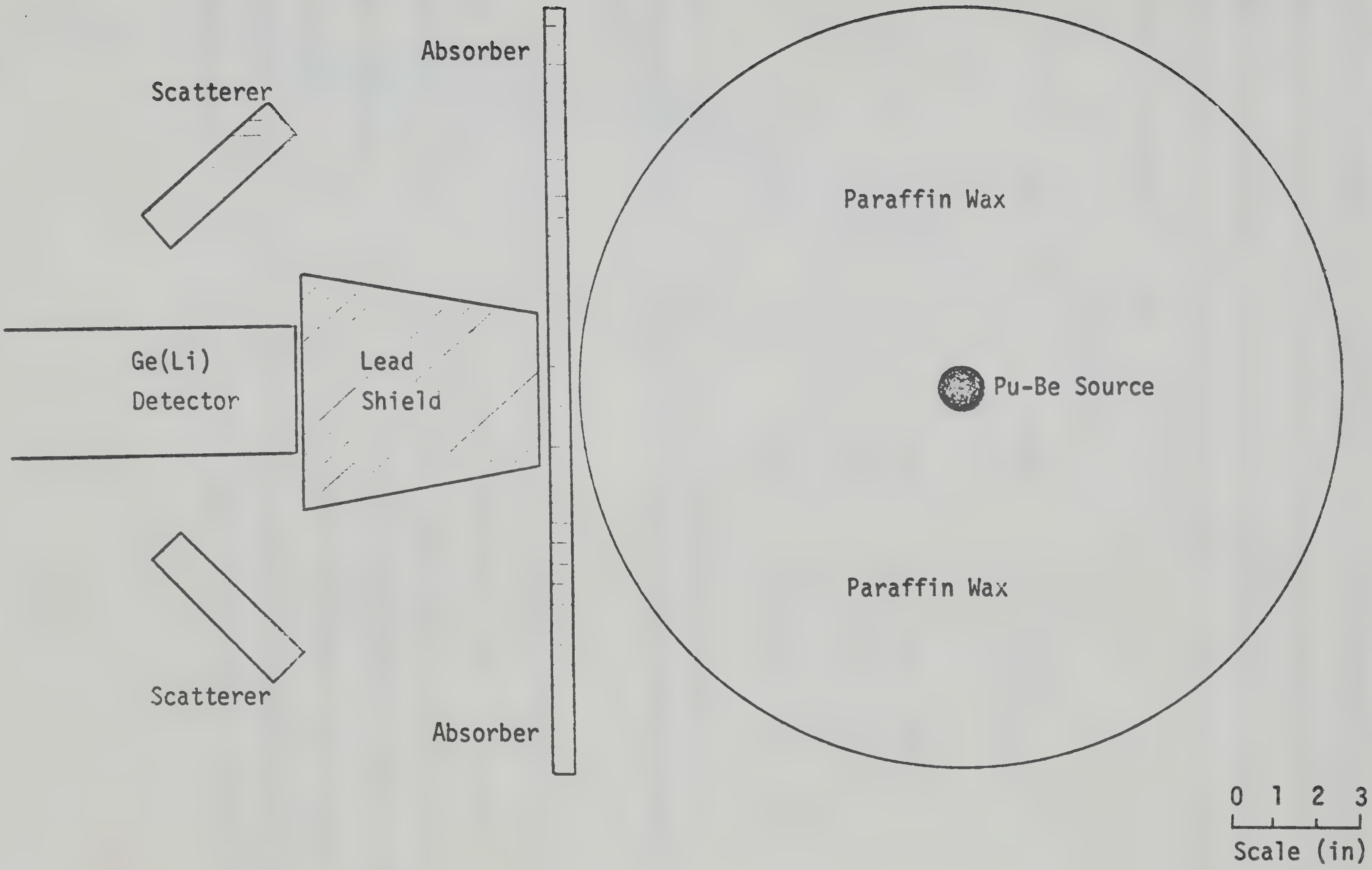

FIG.27. SCHEMMATIC DIAGRAM OF EXPERIMENTAL APPARATUS

copper and iron absorber respectively. The errors quoted are just the statistical errors. It is seen that a very good comparison between the gamma ray attenuation in copper and iron was obtained. In terms of their thicknesses, the attenuation by 1.27cm. of copper was equivalent to that by 1.39 cm. of iron.

SOURCE	ENERGY LEVEL	$\frac{N_{Cu}-N_{Fe}}{N_{Cu}}$ x100%
Cs^{137}	0.66Mev	0.79 ± 0.53%
Co^{60}	1.17Mev	0.15 ± 0.40%
Co^{60}	1.33Mev	1.45 ± 0.41%

Table 3. Results of the gamma ray attenuations obtained for the comparison scatterer iron compared to that of the resonant scatterer copper.

The lead cone in the apparatus was so shaped such that the virtual apex of the cone was at the centre of the source. This lead cone effectively zeroed the number of direct gamma rays to the detector and hence background problems by this means were diminished greatly. Fig.28 shows the spectrum obtained with the lead cone between the plutonium-beryllium source and the detector for the same running time as that for the spectrum obtained in fig.26. The gamma ray reduction is clearly seen.

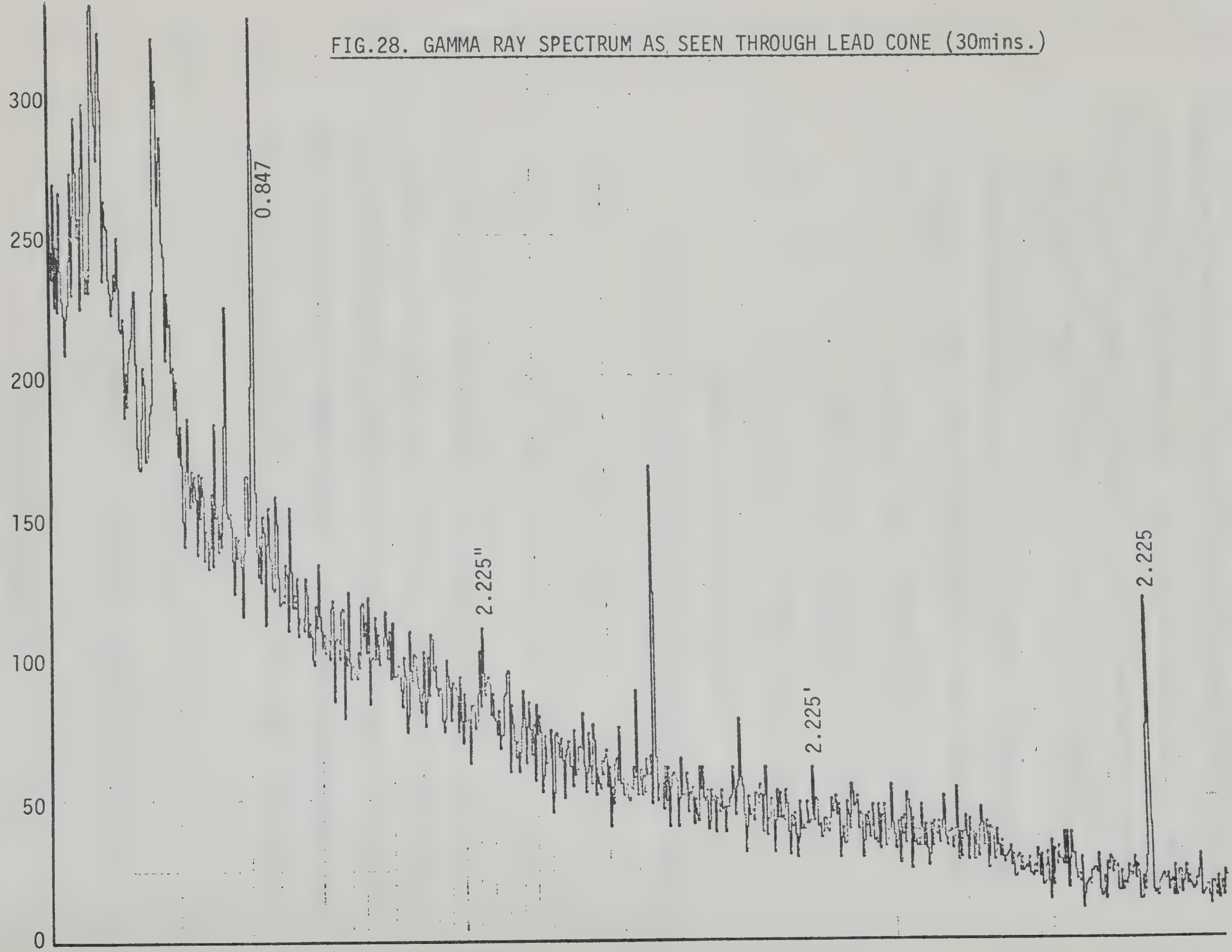

FIG.28. GAMMA RAY SPECTRUM AS SEEN THROUGH LEAD CONE (30mins.)

EXPERIMENTAL PROCEDURE

The resonance self absorption is given by the formula

$$R = \frac{S(0) - S(d)}{S(0)} \qquad 58$$

where S(0) is the number of counts in the peak of interest without the resonant absorber and S(d) is the number of counts in the same peak with a resonant absorber of thickness d inserted between the source and the resonant scatterer. This formula can be made more explicit in terms of the copper and iron scatterers and absorbers as

$$R = \frac{(Cu_{Fe}-Fe_{Fe})-(Cu_{Cu}-Fe_{Cu})}{(Cu_{Fe}-Fe_{Fe})} \qquad 59$$

where the notation for the various experimental runs is;

Cu_{Fe} ≡ copper scatterer, iron absorber
Cu_{Cu} ≡ copper scatterer, copper absorber
Fe_{Fe} ≡ iron scatterer, iron absorber
Fe_{Cu} ≡ iron scatterer, copper absorber.

The subscripts refer to the absorber used in each run. Hence four separate runs are required to obtain the necessary information.

The detector used was a 48c.c. Ge(Li) detector whose preamplifier signal was fed into a Tennelex TC 203BLR amplifier the output of which was then fed into a 2048 channel ADC. This was on line to a 360 Honeywell computer. Each run was stopped after 104000 secs and the spectrum was then 'dumped' from the Honeywell to a SDS

920 computer where it was recorded on magnetic tapes.

Due to the lengthy running times, read outs of the spectrum were taken every 20000secs to check that no electronic gain shifts occurred by observing the relative spacing of the peak points. No such gain shifts were observed in any of the four runs completed. Figs.29 to 32 show the spectrums obtained for the four experimental runs performed. It is noticed that the backgrounds in all are very nearly the same showing that a good comparative attenuation was obtained for the comparison absorber and scatterer, iron.

The Fe_{Fe} run is effectively the background to the Cu_{Fe} run. Fig.33 was obtained by subtracting the spectrum of the Fe_{Fe} run from the Cu_{Fe} run and adding a 1000 counts to each channel. This was done on the SDS computer using a subroutine 'ATOB'. This subtraction eliminates any counts from the resonance peak which may not have occurred by resonance fluorescence as is the case when gamma rays of higher energy than the resonance energy are Compton scattered into the resonance region by the scatterer. Room background is also subtracted out by this method.

Similarly fig.34 shows the subtraction of the effective background run, Fe_{Cu}, from the Cu_{Cu} run. In both figs.33 and 34 the negative peaks are those due to resonance fluorescence effects in the iron comparison scatterer. This was another reason for the choice of iron as the comparison scatterer since its excited energy levels and their decays are off the resonance energy regions for the two copper isotopes.

From the previous figures the energy level configuration of

both Cu^{63} and Cu^{65} can be determined up to 2Mev and these are shown in fig.35.

A neutron monitor gave no reading when placed against the aluminium drum showing that the neutron flux was negligible outside the drum. A more sensitive test on the neutron background was done by placing a slab of copper 5"x5" and 1" thick between the lead cone and the detector. It was assumed that the lead cone would effectively eliminate the gamma flux but not the neutron flux. No scatterer or absorber was used in the run which was 104000secs long. The spectrum obtained was very similar to that of fig.28 with a small indication of the presence of copper peaks. As the gamma flux is in fact not negligible and hence a small amount of resonance fluorescence could occur in the copper it was assumed that any stray neutrons would not affect the results to any appreciable extent.

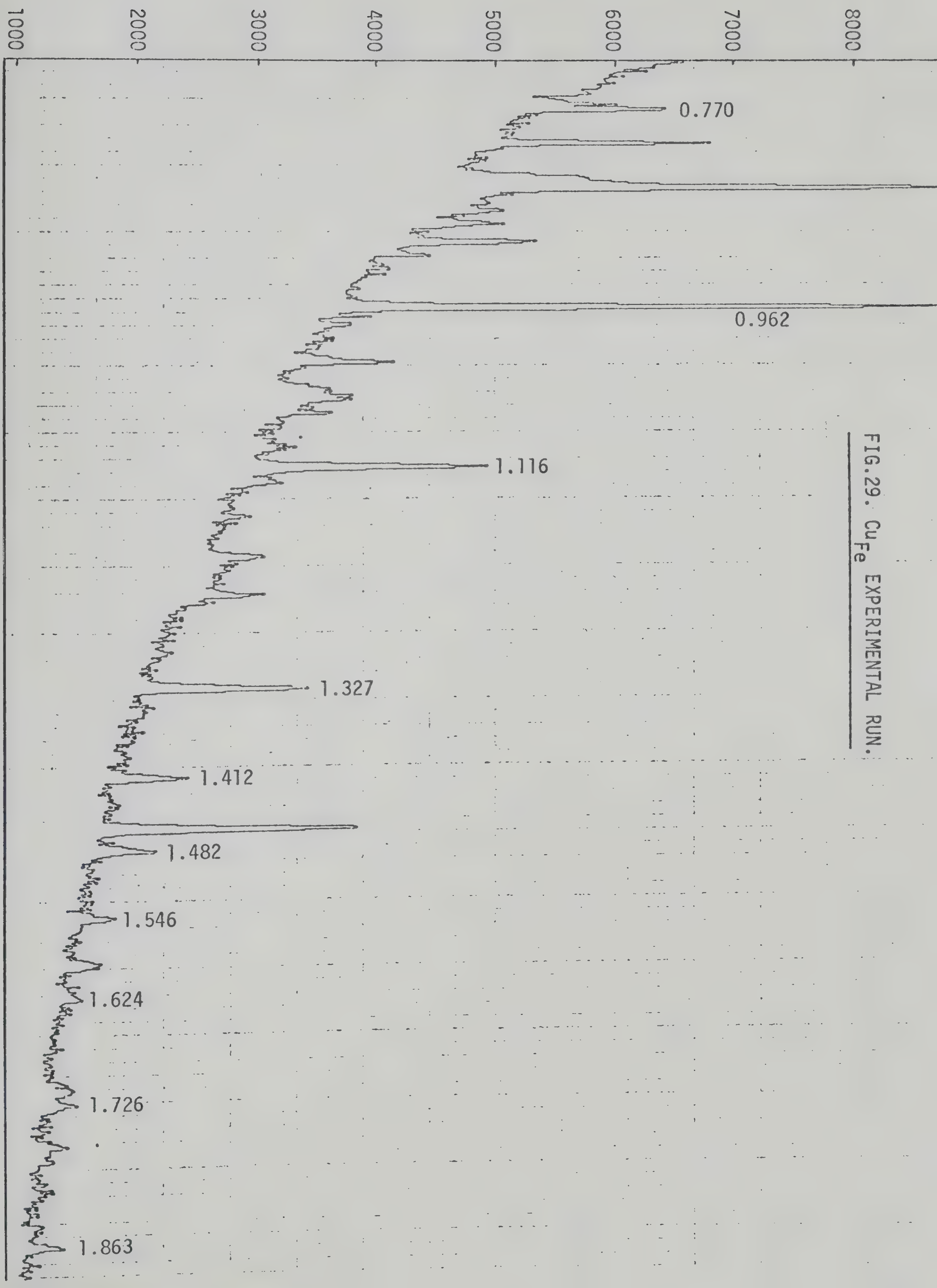

FIG.29. Cu_{Fe} EXPERIMENTAL RUN.

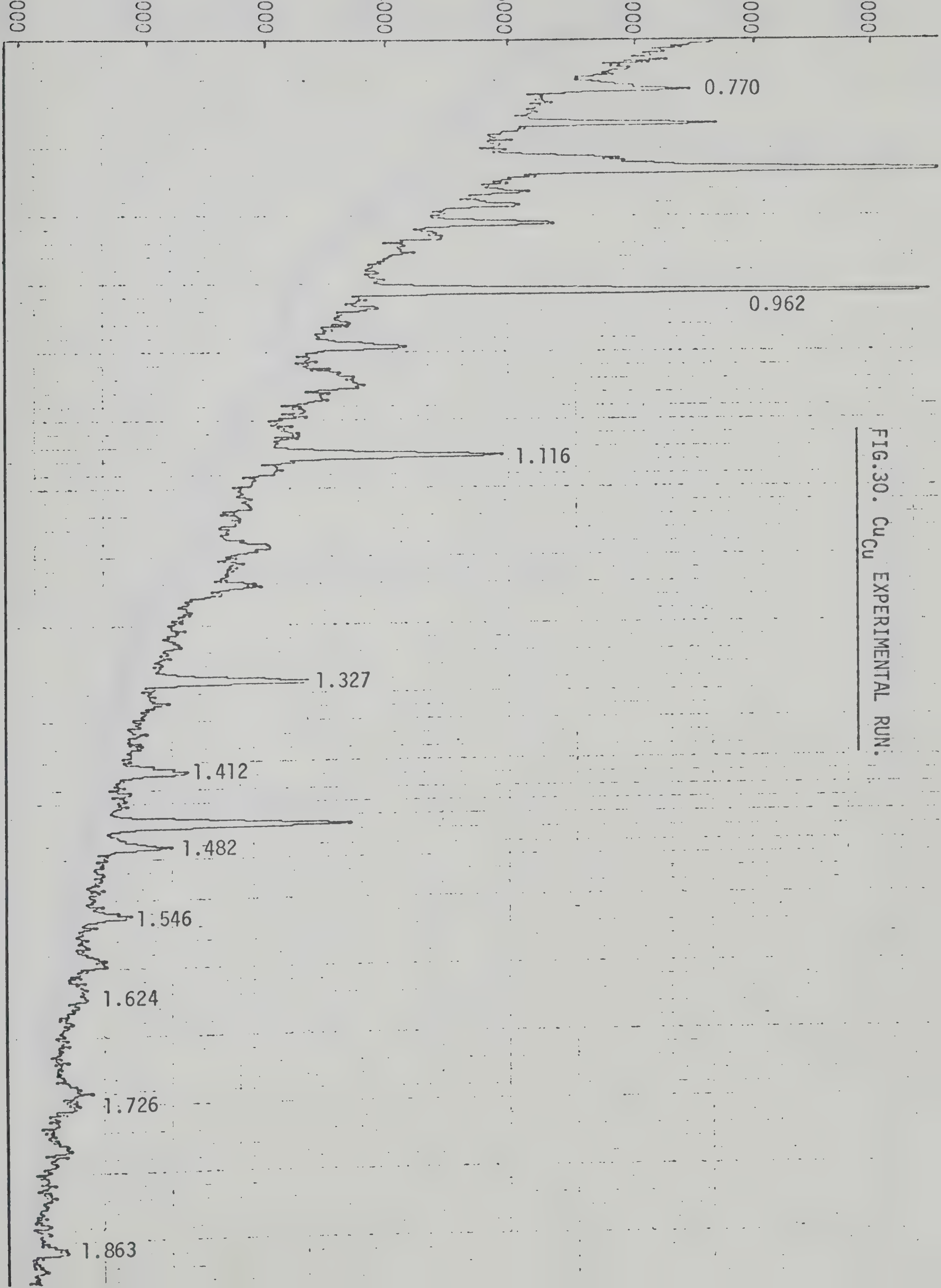

FIG.30. Cu$_{Cu}$ EXPERIMENTAL RUN.

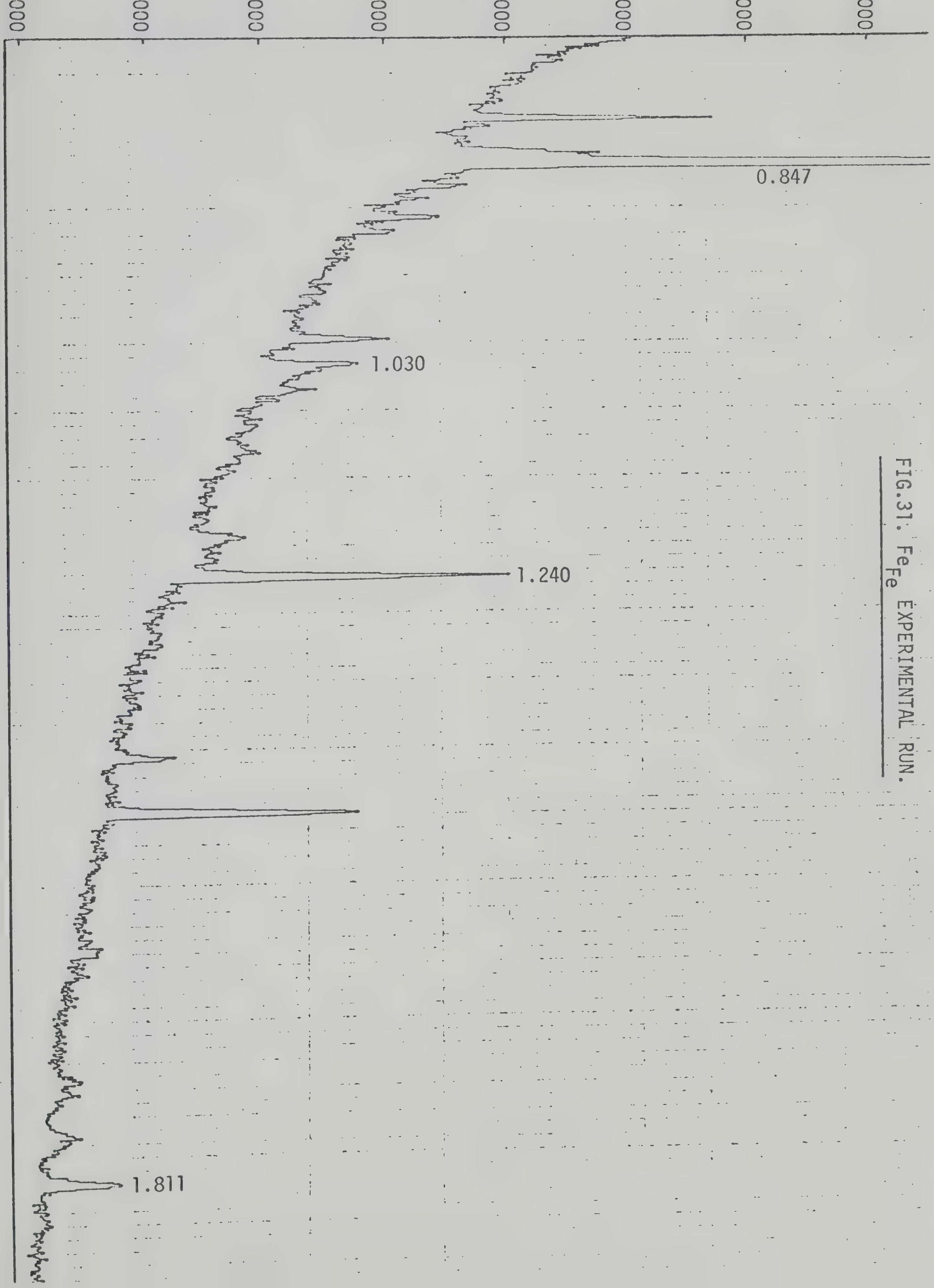

FIG.31. Fe_{Fe} EXPERIMENTAL RUN.

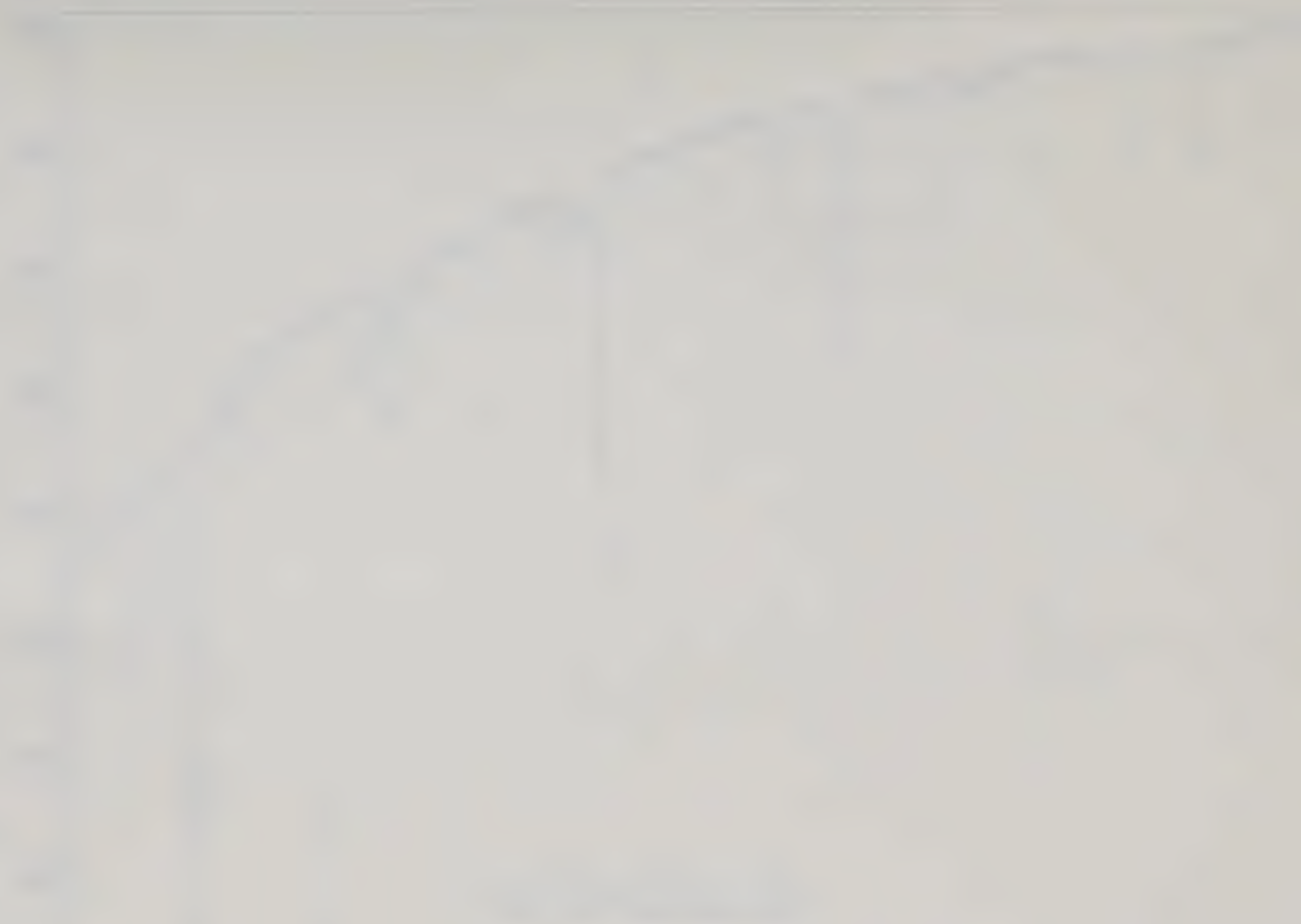

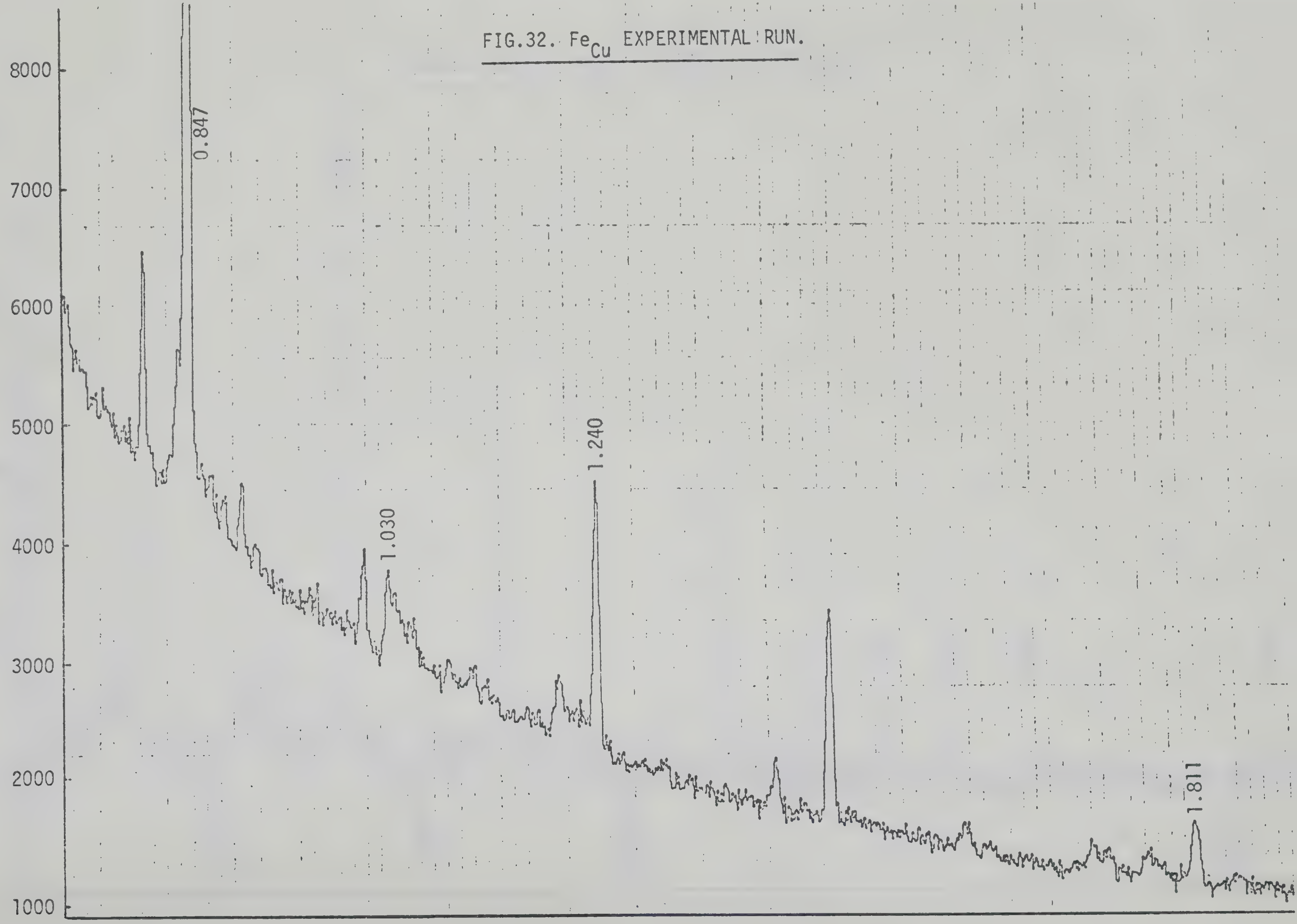

FIG.32. Fe_{Cu} EXPERIMENTAL RUN.

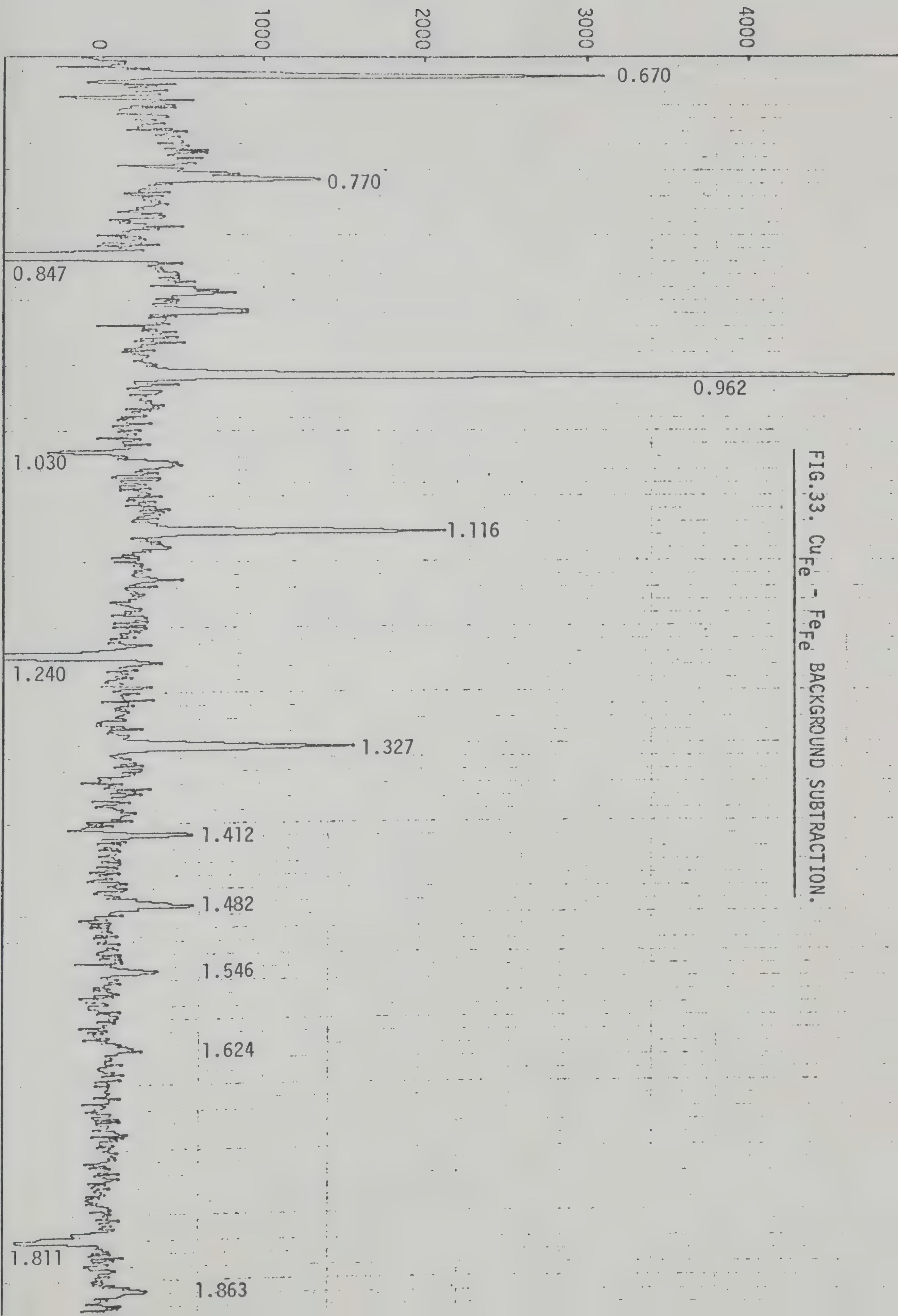

FIG.33. Cu_{Fe} - Fe_{Fe} BACKGROUND SUBTRACTION.

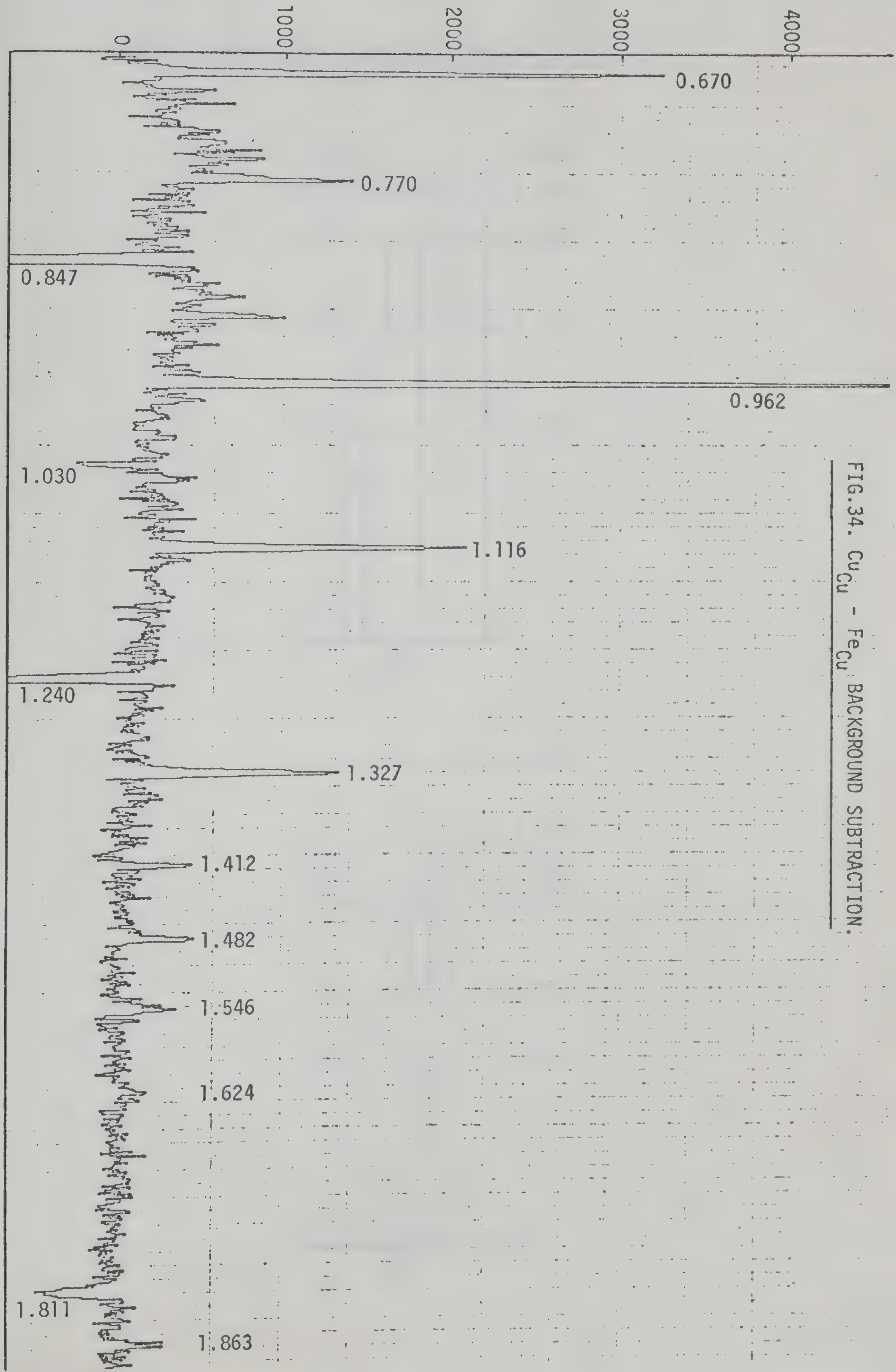

FIG.34. Cu_{Cu} - Fe_{Cu} BACKGROUND SUBTRACTION.

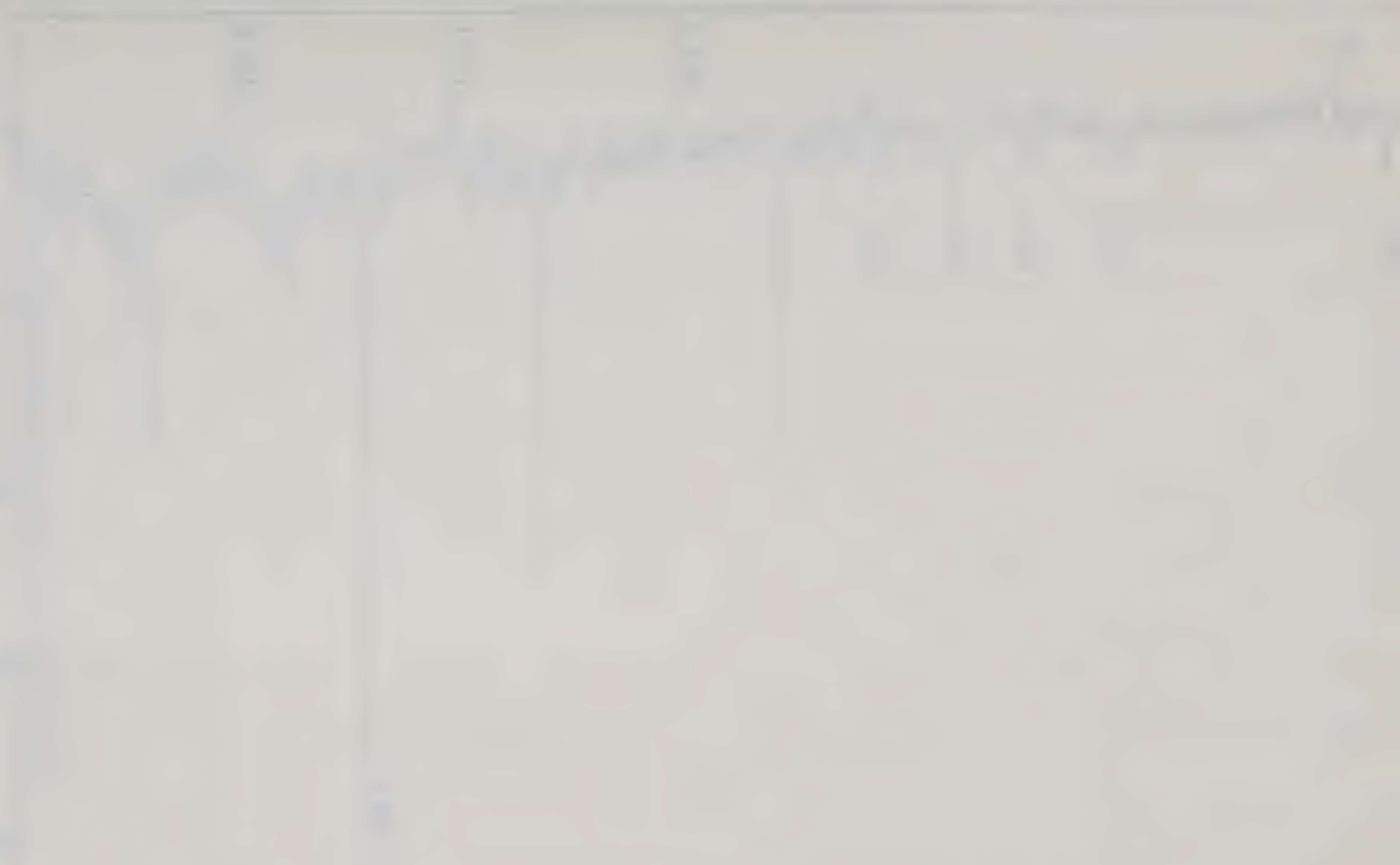

[illegible]

FIG.35. ENERGY LEVEL CONFIGURATIONS OF Cu^{63} AND Cu^{65}.

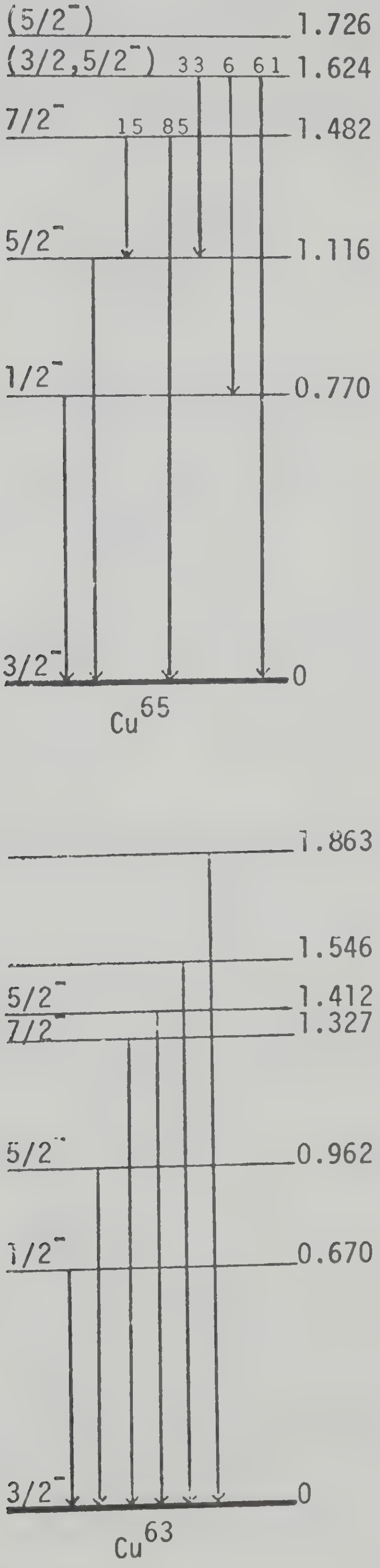

EXPERIMENTAL RESULTS

For the resonance self absorption technique using comparison scatterers and absorbers the formula to be used in the calculation of the nuclear excited level lifetimes is given by eq.39.

$$R = 1 - \exp(-\delta k d)$$

where

$$k = \frac{n\sigma^{0}_{max}\sqrt{\pi}\Gamma}{2\Delta}$$

and n is the number of resonant type nuclei per cm^3 in the resonant scatterer. The Doppler width is given by

$$\Delta = \frac{E}{c}\left[\frac{2KT}{M}\right]^{\frac{1}{2}}$$

where K is Boltzmanns constant. The lifetime of the nuclear level is then given by

$$\tau = \frac{\hbar}{\Gamma}$$

For pure resonance fluorescence where the ground state transition is the only possible means of de-excitation

$$\sigma^{0}_{max} = \frac{\lambda^2}{2\pi} g$$

but for photoexcitation followed by the i^{th} mode of de-excitation

$$\sigma^{0}_{max} = \frac{\lambda^2}{2\pi} g \frac{\Gamma_o \Gamma_i}{\Gamma^2}$$

where g is the ratio $\frac{2J_1 + 1}{2J_o + 1}$.

Since the Doppler width Δ is calculated using the Maxwellian distribution for the velocity distribution of the absorbing nuclei, to make it applicable to solid absorbers Lamb (4) has shown that the absolute temperature T must be replaced by an effective temperature

FIG.36. GRAPH OF THE DEBYE FUNCTION.

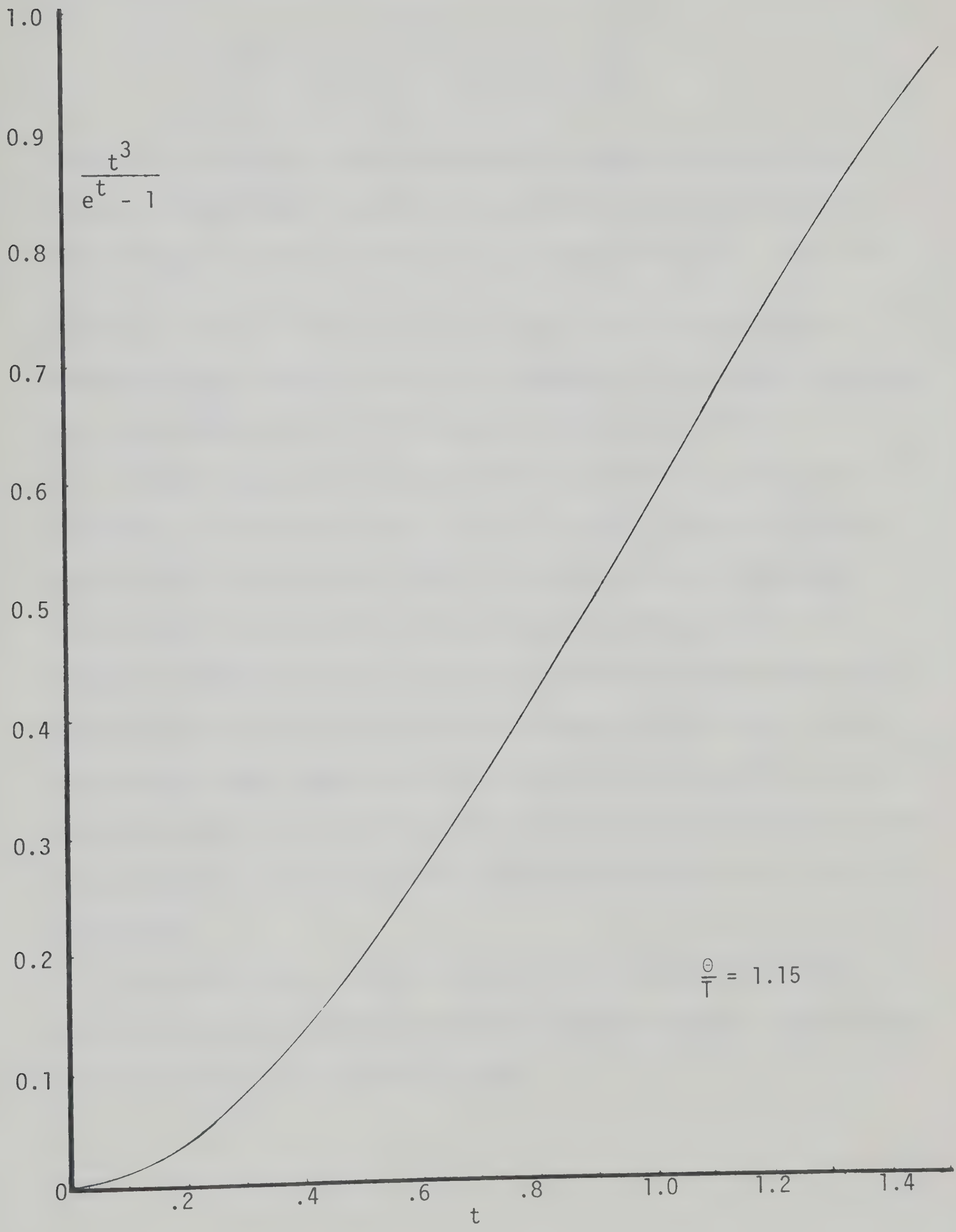

T_{eff} given by the formula

$$\frac{T_{eff}}{T} = 3\left[\frac{T}{\Theta}\right]^3 \int_0^{\frac{\Theta}{T}} t^3\left[\frac{1}{e^t - 1} + \frac{1}{2}\right] dt$$

where Θ is the Debye temperature of the resonant scatterer. This integral is the Debye integral and cannot be calculated by analytic means. Thus in order to calculate T_{eff} a graph of $\frac{1}{e^t - 1}$ vs. t was plotted as shown in fig.36. The area under the curve was found by counting squares and the effective temperature of the copper scatterer at a room temperature of 297°A was calculated to be 317°A.

Table 4 shows the results of the calculations to obtain the lifetimes of the excited levels of Cu^{63} and Cu^{65}. Column two gives the energies of the excited levels as obtained in this experiment and as shown in fig.35. The third column gives the accepted spin changes in de-excitation to the ground state which then leads to the g factor, the ratio of the statistical weights of the spins of the excited and ground states as shown in column four. The fifth column gives the branching ratios from the excited to the ground state and the final column the lifetimes of the respective excited levels given in picoseconds.

The errors shown are the results of the accumulation of the statistical errors involved in the four 'peak-background' subtractions and the one division as given by eq.59.

TABLE 4. EXPERIMENTAL RESULTS

ISOTOPE	ENERGY LEVEL	SPIN CHANGE	$g = \frac{2J_1 + 1}{2J_o + 1}$	$\frac{\Gamma_o}{\Gamma}$	τ (ps)
Cu^{63}	0.670	$\frac{1}{2} \to \frac{3}{2}$	$\frac{1}{2}$	1	0.41 ± 0.11
Cu^{63}	0.962	$\frac{5}{2} \to \frac{3}{2}$	$\frac{3}{2}$	1	1.17 ± 0.30
Cu^{63}	1.327	$\frac{7}{2} \to \frac{3}{2}$	2	1	0.72 ± 0.46
Cu^{63}	1.412	$\frac{5}{2} \to \frac{3}{2}$	$\frac{3}{2}$	1	0.30 ± 0.48
Cu^{65}	0.770	$\frac{1}{2} \to \frac{3}{2}$	$\frac{1}{2}$	1	0.13 ± 0.06
Cu^{65}	1.116	$\frac{5}{2} \to \frac{3}{2}$	$\frac{3}{2}$	1	0.64 ± 0.65
Cu^{65}	1.482	$\frac{7}{2} \to \frac{3}{2}$	2	0.85	0.58 ± 1.73

DISCUSSION

The eleven excited energy levels of the two isotopes of copper, Cu^{63} and Cu^{65}, as obtained in this experiment are in very good agreement with published results. The use of a Ge(Li) detector gave an energy resolution of 1.27 kev/channel which made the identification of the higher energy levels possible. The use of NaI detectors in previous resonance fluorescence experiments made it impossible to consider the extraction of results for the higher energy levels where resonance yields are low.

In this experiment, due to the large statistical errors involved in the 'peak-background' subtractions arising from the small size of the peaks, reliable results could not be obtained for the 1.546 and 1.863Mev levels in Cu^{63} as well as the 1.624 and 1.726Mev levels in Cu^{65}. However, results were obtained for the other levels each of which will be now discussed in turn.

Cu^{63}: 0.670Mev level.

The result obtained of

$$\tau = (4.1 \pm 1.1)\text{x}10^{-13}\text{secs.}$$

is in agreement with other published results. Cumming *et.al.*(27) using the resonance fluorescence technique and the gamma rays from the β decay of a Zn^{63} source as the resonant radiation obtained

$$\tau = (2.94 \pm 0.24)\text{x}10^{-13}\text{secs.}$$

Rothem, Metzger and Swann (28) using gaseous and liquid sources of Zn^{63} obtained the result

$$\tau = (3.1 \pm 0.3)\text{x}10^{-13}\text{secs.}$$

In 1964, Booth, Chason and Wright (29) using the bremsstrahlung technique obtained a lifetime of

$$\tau = (4.3 \pm 1.5)\times10^{-13}\text{secs.}$$

and in 1965 Eswaran *et.al.*(30) using the Doppler Shift Attenuation Method obtained a lifetime of

$$\tau = (3.3 \pm 0.5)\times10^{-13}\text{secs.}$$

Cu^{63}: 0.962Mev level.

This level has also been studied by the above authors and they obtained the following results with the references indicated

$$\tau = (7.2 \pm 1.8)\times10^{-13}\text{secs.} \quad (27)$$

$$\tau = (9.0 \pm 1.5)\times10^{-13}\text{secs.} \quad (28)$$

$$\tau = (9.3 \pm 3.0)\times10^{-13}\text{secs.} \quad (29)$$

$$\tau = (9.6 \pm 0.9)\times10^{-13}\text{secs.} \quad (30)$$

McIntyre and Tandon (25) in their first attempt at using a variable energy source of Compton scattered gamma rays obtained the result

$$\tau = 6 \times 10^{-13}\text{secs}$$

accurate to within a factor of 2. Robinson, McGowan and Stelson (31) measured the lifetime by the Coulomb excitation process and obtained

$$\tau = (6.1 \pm 3.3)\times10^{-13}\text{secs.}$$

Comparing the result obtained in this thesis of

$$\tau = (11.7 \pm 3.0)\times10^{-13}\text{secs.}$$

with the above published results, it is seen to be in agreement with them within the error bars.

Cu^{63}: 1.327Mev level.

In this case Eswaran *et. al.*(30) obtained the lifetime

$$\tau = (8.3 \pm 0.9)\times10^{-13}\text{secs.}$$

and Robinson, McGowan and Stelson (31) the result

$$\tau = (8.7 \pm 1.2)\times10^{-13}\text{secs.}$$

The lifetime for this level was calculated to be

$$\tau = (7.2 \pm 4.6)\times10^{-13}\text{secs.}$$

and is in good agreement with the two above results.

Cu^{63}: 1.412Mev level.

As of yet no data on the lifetime of this level is available and the result obtained of

$$\tau = (3.0 \pm 4.8)\times10^{-13}\text{secs.}$$

establishes the lifetime as being less than 8×10^{-13}secs.

Cu^{65}: 0.770Mev level.

In considering this level account had to be taken of the cascading gamma rays from the 1.624Mev level. However, there is only a 6% branching ratio to the 0.770Mev level from the 1.624Mev level and thus the correction was very small.

Eswaran *et. al.*(30) obtained a lifetime of

$$\tau = (1.3 \pm 0.3)\times10^{-13}\text{secs.}$$

and Booth (21) using the bremsstrahlung technique obtained the value

$$\tau = (1.65 \pm 0.75)\times10^{-13}\text{secs.}$$

Rust *et. al.*(8) using a variable energy source of Compton scattered gamma rays obtained the result

$$\tau = (1.4 \pm 0.5)\times10^{-13}\text{secs.}$$

Hence the value obtained in this thesis of

$$\tau = (1.3 \pm 0.6)\times10^{-13}\text{secs.}$$

is in very good agreement with the above results.

Cu^{65}: 1.116Mev level.

Besides the authors already mentioned, who obtained the results,

$$\tau = (5.3 \pm 0.5)\times10^{-13}\text{secs.} \qquad (30)$$

$$\tau = (9.5 \pm 5.2)\text{x}10^{-13}\text{secs.} \qquad (31)$$

Beard (32) and Kaipov *et. al.*(33), who both used the resonance fluorescence technique obtained the values

$$\tau = (4.4 \pm 1.1)\text{x}10^{-13}\text{secs.}$$

$$\text{and} \qquad \tau = (6.5 \pm 1.6)\text{x}10^{-13}\text{secs.},$$

respectively.The result obtained in this thesis had to be corrected for the gamma rays cascading from the 1.482 and the 1.624Mev levels and the value obtained

$$\tau = (6.4 \pm 6.5)\text{x}10^{-13}\text{secs}$$

is in agreement although the result has a large statistical error.

Cu^{65}: 1.481Mev level.

Although this peak was small its lifetime was calculated but the error is correspondingly large. The result

$$\tau = (5.8 \pm 17.3)\text{x}10^{-13}\text{secs.}$$

approximates the values obtained by Eswaran *et. al.*(30) and Robinson, McGowan and Stelson (31),

$$\tau = (7.6 \pm 1.1)\text{x}10^{-13}\text{secs.}$$

$$\text{and} \qquad \tau = (4.2 \pm 0.9)\text{x}10^{-13}\text{secs.},$$

respectively.

It is surprising that other authors who have used the resonance fluorescence technique to obtain lifetimes using NaI detectors have small statistical errors. It appears that they have only considered the statistical errors involved in two 'peak-background' subtractions i.e. $Cu_{Fe} - Cu_{Cu}$ and $Cu_{Fe} - Fe_{Fe}$, and hence their errors are correspondingly smaller. It is for this reason that a few of the results obtained in this thesis have been stated with errors even though their individual errors are large compared to the result.

The technique described in this thesis is a new method of obtaining nuclear level lifetimes by the resonance fluorescence approach. The method is similar in some ways to the bremsstrahlung technique, however, the effective continuous energy spectrum has a flatter distribution and thus does not suffer the same magnitude of background at the low energy end of the spectrum as is the main problem with the bremsstrahlung technique. This flatness of the spectrum of incident radiation allows a number of nuclear levels to be investigated at the same time. The use of a radioactive source as the means of obtaining the effective continuous energy spectrum replaces the use of an accelerator and hence the method is practicable in almost any laboratory.

Using a Ge(Li) detector a better energy resolution and background subtractions were obtained compared to that obtained in previous resonance fluorescence experiments where NaI detectors were used. Hence the method also affords an accurate means of obtaining the energy levels of the isotope under study. Thus the technique could be used as a useful laboratory experiment for undergraduate students to give them some insight into nuclear physics.

The effective size of the source used in the experiment is the main disadvantage of the method at present. It leads to the use of a large resonant and comparison absorber. Due to the size of these absorbers the number of isotopes that can be studied by the method is limited.

Another problem is the lengthy experimental running times involved since electronic gain shifts must then be considered as well as the percentage increase in the background. A more intense source is preferable to overcome these problems and it would at the same time

lead to better statistical accuracy in the results. Using a more efficient Compton scatterer i.e. one with a large Compton to absorption ratio, with an intense source would lead to a smaller effective source size and hence to a smaller resonant and comparison absorber.

However, when one compares the problems of the other resonance fluorescence techniques, such as the thermal, centrifuge and Compton scattering methods, with those of the technique described in this thesis and when one also considers the simplicity and the intrinsic accuracy of the method, it could well become extensively used in the future as a 'tool' to study nuclear lifetimes by the resonance fluorescence technique.

REFERENCES

1) H. A. Bethe, G. Placzek Phys. Rev. 51 (1937) 450

2) H. A. Bethe Rev. of Modern Phys. 9 (1937) 71

3) E. Melkonian, W. W. Havens, L. J. Rainwater Phys. Rev. 92 (1953) 702

4) W. E. Lamb Phys. Rev. 55 (1939) 190

5) E. Pollard, D. E. Alburger Phys. Rev. 74 (1948) 926

6) S. Ofer, A. Schwarzschild Phys. Rev. 116 (1959) 725

7) F. R. Metzger Progress in Nucl. Phys. 7 (1959) 53

8) N. J. A. Rust *et. al.* Nucl. Inst. and Methods 67 (1969) 222

9) P. B. Smith, P. M. Endt Phys. Rev. 110 (1958) 397

10) G. V. von Dardel, R. Persson Nature 170 (1952) 1117

11) K. G. Malmfors Arkiv for Fysik 6 (1953) 49

12) F. R. Metzger Phys. Rev. 101 (1956) 286

13) P. B. Moon Proc. Phys. Soc. (London) A64 (1951) 76

14) F. R. Metzger, H. Langhoff Phys. Rev. 132 (1963) 1753

15) N. G. Davey, P. B. Moon Proc. Phys. Soc. (London) A66 (1953) 956

16) C. P. Swann, F. R. Metzger Phys. Rev. 108 (1957) 982

17) F. R. Metzger, C. P. Swann, V. K. Rasmussen Phys. Rev. 110 (1958) 906

18) P. B. Smith, P. M. Endt Phys. Rev. 110 (1958) 1442

19) E. Hayward, E. G. Fuller Phys. Rev. 106 (1957) 991

20) O. Beckman, R. Sandstrom Nucl. Phys. 5 (1958) 595

21) E. C. Booth Nucl. Phys. 19 (1960) 426

22) E. C. Booth, K. A. Wright Nucl. Phys. 35 (1962) 472

23) A. M. Cormack Phys. Rev. 96 (1954) 716

24) W. L. Mouton *et. al.* Phys. Rev. 129 (1963) 361

25) G. K. Tandon, J. A. McIntyre Phys. Letters 4 (1963) 117

26) G. K. Tandon, J. A. McIntyre Nucl. Inst. and Meth. 59 (1968) 181

27) J. B. Cumming, A. Schwarzschild, A. W. Sunyar, N. T. Porile Phys. Rev. 120 (1960) 2128

28) T. Rothem, F. R. Metzger, C. P. Swann Nucl. Phys. 22 (1961) 505

29) E. C. Booth, B. Chason, K. A. Wright Nucl. Phys. 57 (1964) 403

30) M. A. Eswaran, H. E. Gove, A. E. Litherland, C. Broude Nucl. Phys. 66 (1965) 401

31) R. L. Robinson, F. K. McGowan, P. H. Stelson Phys. Rev. 134 (1964) B567

32) G. B. Beard Phys. Rev. 135 (1964) B577

33) D. K. Kaipov, R. B. Begzhanov, A. V. Kuziminov, Yu. K. Shubnyi Soviet Phys. JEPT 17 (1963) 1217

SUPPLEMENTARY REFERENCES FOR THE THEORETICAL SECTION

F. R. Metzger Phys. Rev. 103 (1956) 983

F. R. Metzger Phys. Rev. 110 (1958) 123

S. Ofer, A. Schwarzschild Phys. Rev. 116 (1959) 725

F. R. Metzger Phys. Rev. 127 (1962) 220

F. R. Metzger Phys. Rev. 137 (1965) 1415